ACS Catalysis

Review

pubs.acs.org/acscatalysis

Z-Scheme Water Splitting Using Two Different Semiconductor Photocatalysts

Kazuhiko Maeda*,†,‡

†Department of Chemistry, Graduate School of Science and Engineering, Tokyo Institute of Technology, 2-12-1-NE-2 Ookayama, Meguro-ku, Tokyo 152-8550, Japan

‡Precursory Research for Embryonic Science and Technology (PRESTO), Japan Science and Technology Agency (JST), 4-1-8 Honcho Kawaguchi, Saitama 332-0012, Japan

ABSTRACT: Water splitting on illuminated semiconductors has long been studied as a potential means of converting solar energy into chemical energy in the form of H_2, a clean and renewable energy carrier. Photocatalytic water splitting through two-step photoexcitation using two different semiconductor powders and a reversible donor/acceptor pair (so-called shuttle redox mediator) is one of the possible forms of artificial photosynthesis. This system was inspired by natural photosynthesis in green plants and is called the "Z-scheme". The development of Z-scheme water splitting systems has relied on both finding a new semiconductor photocatalyst that efficiently works in the presence of a shuttle redox mediator and creating active sites to promote surface chemical reactions while suppressing backward reactions involving redox mediators. This review article describes the historical development of photocatalytic water splitting systems driven by the Z-scheme principle.

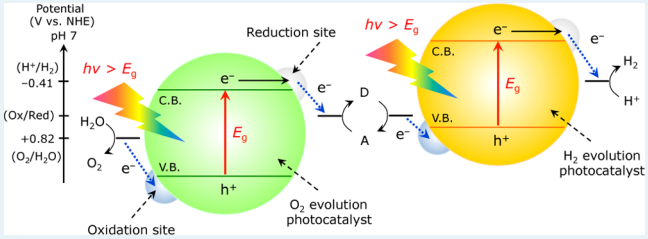

KEYWORDS: *artificial photosynthesis, electron relay, heterogeneous photocatalysis, hydrogen evolution, light energy conversion, solar fuel, water oxidation*

1. INTRODUCTION

1.1. Research Background. Catalytic water splitting into H_2 and O_2 in the presence of a semiconductor powder with visible light is a promising approach for storing solar energy as chemical energy.[1−13] The reaction (eq 1) is a typical "uphill reaction", involving a large positive change in the Gibbs energy (ΔG° = 237.13 kJ mol^{-1}).

$$2H_2O \rightarrow 2H_2 + O_2 \quad (1)$$

Research in this field was initially triggered by the demonstration of photoelectrochemical water splitting using a single-crystal titanium dioxide (rutile) photoanode and a Pt cathode with a chemical bias.[14] This is well-known as the Honda−Fujishima effect. Overall water splitting for the production of H_2 using a semiconductor particle has been under investigation since 1980[15−17] and has been extensively studied by many researchers. From the viewpoint of large-scale H_2 production, particulate photocatalyst systems have a wider range of potential applications, although a method for separating the simultaneously produced H_2 and O_2 remains to be developed.[6] Because the main component of the solar spectrum (~50%) consists of visible light ($400 < \lambda < 800$ nm), a primary goal in photocatalytic water splitting is to efficiently utilize visible light to achieve the reaction.

1.2. Basic Principle of Photocatalytic Water Splitting by One-Step Photoexcitation. Figure 1 shows a schematic illustration of the basic principle of overall water splitting on a semiconductor particle. Under irradiation with energy equivalent to or greater than the band gap of the semiconductor photocatalyst, electrons in the valence band are excited into the conduction band, leaving holes in the valence band. These photogenerated electrons and holes cause reduction and oxidation reactions, respectively. To achieve overall water splitting, the bottom of the conduction band must be more negative than the reduction potential of H^+ to H_2 (−0.41 V vs NHE at pH 7), and the top of the valence band must be more

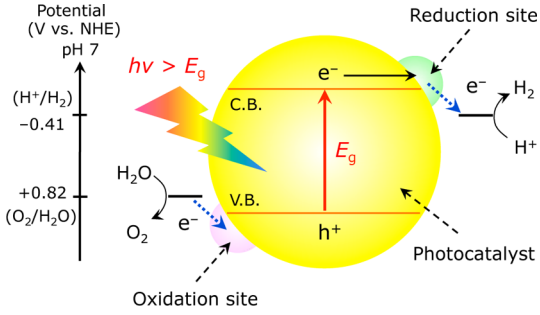

Figure 1. Schematic energy diagram of photocatalytic water splitting for a one-step photoexcitation system. C.B., conduction band; V.B., valence band; E_g, band gap. Reproduced from ref 6 with permission. Copyright 2010, American Chemical Society.

Received: March 19, 2013
Revised: May 20, 2013
Published: May 21, 2013

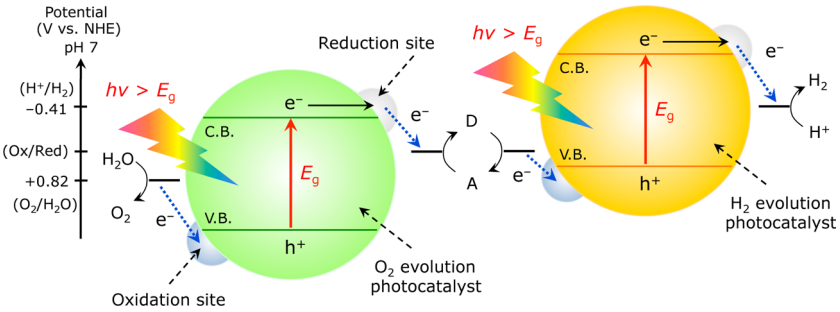

Figure 2. Schematic energy diagram of photocatalytic water splitting for a two-step photoexcitation system. C.B., conduction band; V.B., valence band; E_g, band gap. D and A indicate electron donating and accepting species, respectively. Reproduced from ref 6 with permission. Copyright 2010, American Chemical Society.

positive than the oxidation potential of H_2O to O_2 (0.82 V vs NHE at pH 7). Therefore, the minimum photon energy thermodynamically required to drive the reaction is 1.23 eV, which corresponds to a wavelength of ~1000 nm, in the near-infrared region. Accordingly, it would appear possible to utilize the entire spectral range of visible light ($400 < \lambda < 800$ nm); however, there is an activation barrier in the charge transfer process between the photocatalyst and water molecules, necessitating a photon energy greater than the band gap of the photocatalyst to drive the overall water-splitting reaction at a reasonable rate. In addition, the backward reaction, that is, water formation from H_2 and O_2, must be strictly inhibited, and the photocatalysts themselves must be stable in the reaction. Furthermore, although there are a large number of materials that possess suitable band gap potentials, there are very few that function as a photocatalyst for overall water splitting due to as a result of other factors that will be discussed below.

The major obstacle to progress in the development of a photocatalyst driven by one-step photoexcitation has been the lack of a suitable compound that meets the following three requirements: (1) a band gap narrower than 3 eV, (2) band-edge potentials suitable for overall water splitting, and (3) stability in the photocatalytic reaction.[2] Metal oxides have been extensively studied as photocatalysts for one-step water splitting, and some have achieved high quantum efficiencies as high as several tens of percent;[4] however, the tops of the valence bands of such metal oxide photocatalysts, having d^0 or d^{10} metal cations, usually consist of O2p orbitals, which are located at ~+3 V or higher (vs NHE). Therefore, if the bottom of the conduction band of a given metal oxide is located at a potential more negative than the water reduction potential, the band gap of the material will inevitably become larger than 3 eV, rendering the material inactive in the visible-light region.[18] A few chalcogenides and metal oxides (e.g., CdS and WO_3)[19−23] are known to be photocatalytically active under visible light. Certain metal chalcogenides, including CdS and CdSe, appear to be suitable photocatalysts for overall water splitting, exhibiting band gap energies sufficiently small to allow absorption of visible light and having conduction and valence bands at potentials appropriate for water reduction and oxidation. These metal chalcogenides, however, are not stable in water oxidation reaction to form O_2 because the S^{2-} and Se^{2-} anions are more susceptible to oxidation than water, causing the CdS or CdSe catalyst itself to be oxidized and degraded.[19,20] Although WO_3 functions as a stable photocatalyst for O_2 evolution under visible light in the presence of an appropriate electron acceptor as discussed in the latter sections,[21−23] the bottom of the conduction band of the material is located at a more positive potential than the potential of water reduction. As a result, WO_3 does not have the ability to reduce H^+ to H_2. Until very recently, reproducible photocatalytic systems for visible-light-driven overall water splitting had not been realized,[8] although there are several reports that claimed to demonstrate the decomposition of water under visible light. Therefore, one-step water splitting by visible light had been once described as one of the "Holey Grails" of chemistry.[24]

1.3. Processes of Z-Scheme Water Splitting on Semiconductor Photocatalysts. In the development of visible-light-driven photocatalysts for one-step water splitting, another approach to achieve water splitting with visible light was originally introduced by Bard in 1979.[25] This system was inspired by natural photosynthesis in green plants, where the photosystems I and II harvest 700 and 680 nm photons, respectively, oxidizing H_2O into O_2 under sunlight, with a quantum yield close to unity. In this system (the so-called Z-scheme), two different photocatalysts are combined using an appropriate shuttle redox mediator. Visible light can be utilized more efficiently than in the conventional one-step water-splitting systems because the energy required to drive each photocatalyst is reduced. It is also possible to apply a photocatalyst that has either water reduction or oxidation potential to one side of the system. For example, WO_3, that does not have the ability to reduce H^+, is capable of producing O_2 from an aqueous solution containing appropriate electron acceptors under visible light and acts as an effective building block for O_2 evolution in Z-scheme water splitting, as will be discussed in detail later.

A schematic illustration of Z-scheme water splitting is shown in Figure 2. In a H_2 evolution system, the forward reactions that should occur on the photocatalyst surface are the reduction of protons by conduction band electrons and the oxidation of an electron donor (D) by valence band holes to yield the corresponding electron acceptor (A), as follows:

$$2H^+ + 2e^- \rightarrow H_2 \quad (\text{photoreduction of } H^+ \text{to } H_2) \tag{2}$$

$$D + nh^+ \rightarrow A \quad (\text{photooxidation of D to A}) \tag{3}$$

On the other hand, the forward reactions on an O_2 evolution photocatalyst are as follows,

$$A + ne^- \rightarrow D \quad (\text{photoreduction of A to D}) \tag{4}$$

$$2H_2O + 4h^+ \rightarrow O_2 + 4H^+ \quad (\text{photooxidation of } H_2O \text{ to } O_2) \tag{5}$$

dx.doi.org/10.1021/cs4002089 | ACS Catal. 2013, 3, 1486−1503

where the electron acceptor generated by the paired H_2 evolution photocatalyst is converted to its reduced form (D), and water oxidation occurs with the valence band holes. Thus, a cycle of redox pairs (D and A) occurs, and the water-splitting reaction is achieved.

1.4. Factors Affecting Activity. As shown in Figure 3, photocatalytic reaction, here taking one-step water splitting for

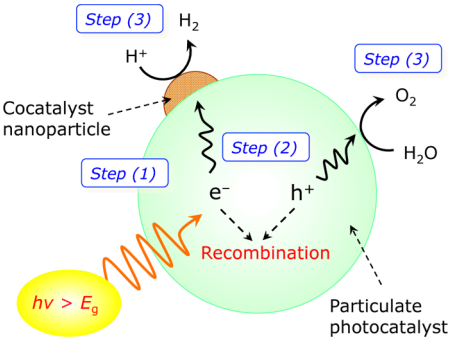

Figure 3. Processes involved in photocatalytic overall water splitting on a semiconductor particle. E_g indicates the band gap energy of a photocatalyst. Reproduced from ref 2 with permission. Copyright 2007, American Chemical Society.

example, on a semiconductor photocatalyst (typically of submicrometer size) occurs in three steps: (1) the photocatalyst absorbs photon energy greater than the band gap energy of the material and generates photoexcited electron–hole pairs in the bulk, (2) the photoexcited carriers separate and migrate to the surface without recombination, and (3) water molecules (or H^+) are reduced and oxidized by the photogenerated electrons and holes to produce H_2 and O_2, respectively.[2,8] The first two steps are strongly dependent on the structural and electronic properties of the photocatalyst. In general, high crystallinity has a positive effect on activity, since the density of defects, which act as recombination centers between photogenerated carriers, decreases with increasing crystallinity. Higher photocatalytic activity can also be expected by reducing the particle size of a photocatalyst because the diffusion length for photogenerated electron–hole pairs can be shortened. The third step, on the other hand, is promoted by the presence of a solid cocatalyst. The cocatalyst is typically a noble metal (e.g., Pt, Rh) or transition-metal oxide (e.g., NiO_x, RuO_2) and is loaded onto the photocatalyst surface as a dispersion of nanoparticles (typically ranging from 1 to 50 nm in size) to produce active sites and reduce the activation energy for surface chemical reactions. In most cases, cocatalysts are loaded for the promotion of H_2 evolution, presumably because most photocatalysts do not offer an active site for catalytic H_2 evolution on the surface. For Z-scheme water splitting, loading cocatalysts of course plays an essential role in constructing active sites for photoredox reactions, as will be discussed later. It is thus important to design both the bulk and surface properties of the material carefully so as to obtain a high activity for the water-splitting reaction.

Controlling the selectivity of chemical reactions that occur on the photocatalyst surface during Z-scheme water splitting is also an important research subject. As shown in Figure 2, the reduction of A and oxidation of D are, respectively, more likely to occur on H_2 and O_2 evolution photocatalysts than water reduction and oxidation. For this reason, the number of Z-scheme water-splitting systems showing a reasonable level of activity under visible light is limited, even though a large number of visible-light-responsive photocatalysts have been developed.[4]

The performance of a given photocatalytic material should ideally be evaluated on the basis of quantum yield. However, it is almost impossible to measure the real quantum yield of a powder-based photocatalytic system for water splitting. The main obstacle is the lack of a suitable method of evaluating the loss of incident photons by scattering and reflection in a particulate suspension. In other words, there is no reliable means of determining the number of photons absorbed by the photocatalyst particles. Therefore, a quantum yield of a given photocatalyst for water splitting is evaluated, without exception, as an apparent (or external) quantum yield (AQY), in which all of the incident photons are assumed to be absorbed in a given photocatalyst suspension. AQY can be estimated as

$$\mathrm{AQY}(\%) = (A \times R)/I \times 100 \quad (6)$$

where A, R, and I represent coefficients based on the reactions (H_2 evolution, 4; O_2 evolution, 8), the H_2 or O_2 evolution rate, and the rate of incident photons, respectively. The flux of incident photons is typically measured using a calibrated photodiode or chemical actinometry.

1.5. Scope of this Review Article. So far, some review papers on Z-scheme water splitting that focus on specific aspects have already been available.[9,10] A thoughtful review paper on water splitting using particulate photocatalysts, which covers fundamental concepts and experimental methods for water splitting including Z-scheme, has been published by Kudo and Miseki.[4] To the author's knowledge, however, no review paper that deals with the historical development of Z-scheme water-splitting photocatalysts has been reported.

In the next section, the history of the development of semiconductor photocatalysts for Z-scheme water splitting is introduced, then the effects of redox mediators and cocatalysts in Z-scheme water splitting on the efficiency are discussed. Finally, the future outlook for research in this field is discussed. The available combinations active for Z-scheme water splitting into H_2 and O_2, which will be discussed below, are in advance summarized in Table 1. In addition, the reduction and oxidation potentials of water and several shuttle redox couples are listed in Table 2.

2. DEVELOPMENT OF SEMICONDUCTOR PHOTOCATALYSTS APPLICABLE TO Z-SCHEME WATER SPLITTING

2.1. Early Works. Water oxidation using oxide semiconductors such as TiO_2 and WO_3 in the presence of Fe^{3+} as an electron acceptor (an O_2 evolution half reaction of Z-scheme water splitting) was first reported by Kransnovskii et al. in 1962.[21] Darwent and Mills reported that the O_2 evolution rate from an aqueous solution containing Fe^{3+} under visible light ($400 < \lambda < 450$ nm) was enhanced by deposition of RuO_2 on the surface of WO_3.[22] Grätzel et al. compared the ability of Fe^{3+} to accept electrons from the conduction band of WO_3 with that of Ag^+ as an irreversible electron acceptor.[23] By observing O_2 generated, they found that the latter is much better than the former. The AQYs for Fe^{2+} and O_2 production achieved in these early works were below 0.4% at 405 nm.

For H_2 evolution side, Mallouk et al. in 1991 achieved visible-light photolysis of hydrogen iodide (HI) that stores light energy into chemical energy in the form of H_2 and I_3^- using Pt-intercalated $H_2K_2Nb_4O_{17}$ sensitized by a ruthenium com-

dx.doi.org/10.1021/cs4002089 | ACS Catal. 2013, 3, 1486–1503

Table 1. Summary of Z-Scheme Water Splitting Systems That Have Been Reported So Far

	photocatalyst (available wavelength)				
entry	H_2	O_2	redox mediator	max apparent quantum yield/%	ref (year)
1	Fe^{2+} (<280 nm)	RuO_2/WO_3 (<460 nm)	Fe^{3+}/Fe^{2+}	no data	32 (1997)
2	Pt/TiO_2 anatase (<380 nm)	TiO_2 rutile (<410 nm)	IO_3^-/I^-	1 (350 nm)	33 (2001)
3	$Pt/SrTiO_3$:Cr/Ta (<550 nm)	PtO_x/WO_3 (<460 nm)	IO_3^-/I^-	1 (420 nm)	35−37 (2001)
4	$Pt/SrTiO_3$:Bi/Ga (<370 nm)	$SrTiO_3$:In/V (<370 nm)	IO_3^-/I^-	no data	49 (2012)
5	$Pt/SrTiO_3$:Rh (<520 nm)	Ru/$SrTiO_3$:In/V (<520 nm)	IO_3^-/I^-	0.33 (360 nm) 0.056 (420 nm) 0.039 (480 nm)	50 (2012)
6	$Pt/SrTiO_3$:Cr/Ta (<550 nm)	Cs^+-PtO_x/WO_3 (<460 nm)	IO_3^-/I^-, I_3^-/I^-	no data	41 (2013)
7	coumarin dye-adsorbed $Pt/H_2K_2Nb_6O_{17}$ (<750 nm)	IrO_2-Pt/WO_3 (<460 nm)	I_3^-/I^-	<0.1 (500 nm) for H_2 evolution	39 (2009)
8	Pt/TiO_2 anatase (<400 nm)	NO_3^- (<250 nm)	NO_3^-/NO_2^-	no data	51 (2006)
9	$Pt/SrTiO_3$:Rh (<520 nm)	$BiVO_4$ (<520 nm)	Fe^{3+}/Fe^{2+}	0.4 (420 nm) 0.3 (440 nm)	42 (2004)
10	$Pt/SrTiO_3$:Rh (<520 nm)	Bi_2MoO_6 (<450 nm)	Fe^{3+}/Fe^{2+}	0.2 (440 nm)	42 (2004)
11	$Pt/SrTiO_3$:Rh (<520 nm)	WO_3 (<460 nm)	Fe^{3+}/Fe^{2+}	0.5 (420 nm) 0.2 (440 nm)	42 (2004)
12	Ru/$SrTiO_3$:Rh (<520 nm)	$BiVO_4$ (<520 nm)	Fe^{3+}/Fe^{2+}	0.3 (420 nm)	83 (2008)
13	Ru/$SrTiO_3$:Rh (<520 nm)	$BiVO_4$ (<520 nm)	$[Co(bpy)_3]^{3+/2+}$ or $[Co(phen)_3]^{3+/2+}$	2.1 (420 nm)	52 (2013)
14	Ru/$SrTiO_3$:Rh (<520 nm)	$BiVO_4$ (<520 nm)	none	1.7 (420 nm)	48 (2009)
15	Ru/$SrTiO_3$:Rh (<520 nm)	$Ir/CoO_x/Ta_3N_5$ (<600 nm)	none	no data	75 (2013)
16	Ru/$SrTiO_3$:Rh (<520 nm)	$BiVO_4$ (<520 nm)	none (reduced graphene oxide)	1.03 (420 nm)	76 (2011)
17	Pt/TaON (<520 nm)	PtO_x/WO_3 (<460 nm)	IO_3^-/I^-	0.5 (420 nm)	54, 56 (2005)
18	Pt/TaON (<520 nm)	RuO_2/TaON (<520 nm)	IO_3^-/I^-	0.1 (420−440 nm)	57 (2008)
19	$Pt/CaTaO_2N$ (<520 nm)	PtO_x/WO_3 (<460 nm)	IO_3^-/I^-	no data	59, 60 (2008)
20	$Pt/BaTaO_2N$ (<660 nm)	PtO_x/WO_3 (<460 nm)	IO_3^-/I^-	0.1 (420−440 nm)	59, 60 (2008)
21	Pt/ZrO_2/TaON (<520 nm)	PtO_x/WO_3 (<460 nm)	IO_3^-/I^-	6.3 (420 nm)	62, 65 (2008)
22	Pt/ZrO_2/TaON (<520 nm)	$Ir/TiO_2/Ta_3N_5$ (<600 nm)	IO_3^-/I^-	no data	71 (2010)
23	Pt/ZrO_2/TaON (<520 nm)	RuO_2/TaON (<520 nm)	IO_3^-/I^-	no data	58 (2011)
24	$Pt/BaZrO_3-BaTaO_2N$ (<660 nm)	PtO_x/WO_3 (<460 nm)	IO_3^-/I^-	0.6 (420−440 nm)	67, 69 (2011)
25	$Pt/BaZrO_3-BaTaO_2N$ (<660 nm)	TiO_2 rutile (<410 nm)	Fe^{3+}/Fe^{2+}	no data	69 (2013)

Table 2. The Reduction and Oxidation Potentials of Water and Several Shuttle Redox Mediators

reaction	potential vs NHE/V
$2H^+ + 2e^- = H_2$	0−0.059 × pH
$Co(bpy)_3^{3+} + e^- = Co(bpy)_3^{2+}$	0.30[a]
$Co(phen)_3^{3+} + e^- = Co(phen)_3^{2+}$	0.36[a]
$I_3^- + 2e^- = 3I^-$	0.536
$Fe^{3+} + e^- = Fe^{2+}$	0.771
$N_2O_4 + 2e^- = 2NO_2^-$	0.867
$IO_3^- + 6e^- + 3H_2O = I^- + 6OH^-$	1.085−0.059 × pH
$2H_2O + 4e^- = O_2 + 4H^+$	1.229−0.059 × pH

[a]Data from Krishnan et al.[26]

plex.[27,28] The intercalated Pt nanoparticles are most likely to work as H_2 evolution sites by suppressing the access of I_3^- ions, which are more susceptible to reduction than protons, owing to the layered architecture that consists of negatively charged niobate sheets. However, the H_2 evolution rate gradually decreased with reaction time, as shown in Figure 4. Because no dark reaction between H_2 and I_3^- occurred, the deactivation was attributable to the reduction of the accumulated I_3^- by electrons from the surface of $H_2K_2Nb_4O_{17}$. The photolysis of HI on sensitized $H_2K_2Nb_4O_{17}$ particles is schematically illustrated in Figure 5. Matsumura et al. performed the same reaction but with Pt-loaded anatase TiO_2 as a photocatalyst under UV irradiation ($\lambda > 300$ nm).[29] In this case, however, H_2 evolution also ceased due to the backward reaction involving I_3^-. A follow-up study by Mallouk et al. demonstrated that modification of the Ru-sensitized $H_2K_2Nb_4O_{17}$ particles with either $[TiNbO_5]_n^{n-}$ polyanions (derived from exfoliated $HTiNbO_5$) or poly(styrenesulfonate), which repel negatively charged ions like I_3^-, showed 3−5 times improvement in H_2 evolution activity as a result of a decrease in the rate of back electron transfer from the $H_2K_2Nb_4O_{17}$ component to I_3^- ions. As a result, an initial AQY of ∼3% at 450 ± 50 nm was obtained,[30] an order of magnitude higher than the previously reported value (∼0.3%).[27,28]

The results of HI photolysis suggested the possibility of creating a sustainable energy conversion photosystem if the reactions can be coupled with a certain water oxidation system that can reduce an electron-accepting species such as I_3^-.

dx.doi.org/10.1021/cs4002089 | ACS Catal. 2013, 3, 1486−1503

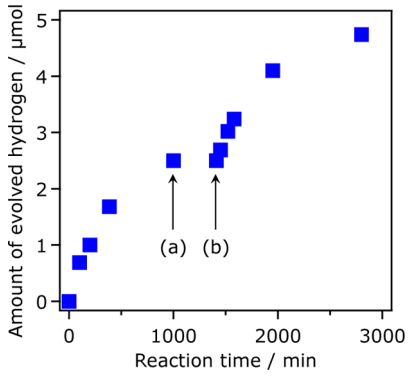

Figure 4. Photochemical H_2 evolution from 100 mg of Pt (0.05%)-intercalated $K_{4-x}H_xNb_6O_{17}\cdot nH_2O$ sensitized by a ruthenium complex (5×10^{-7} mol g^{-1}) in 8.0 mL of 50 mM aqueous KI solution (pH 3.0). Irradiation was interrupted at point (a), and a gas sample was taken at point (b) to check for recombination of H_2 and I_3^-; the sample was filtered, and irradiation was continued in a fresh 50 mM KI solution. Light source: filtered Hg–Xe lamp, intensity 24 mW, λ = 450 ± 50 nm. Reproduced from ref 27 with permission. Copyright 1991, American Chemical Society.

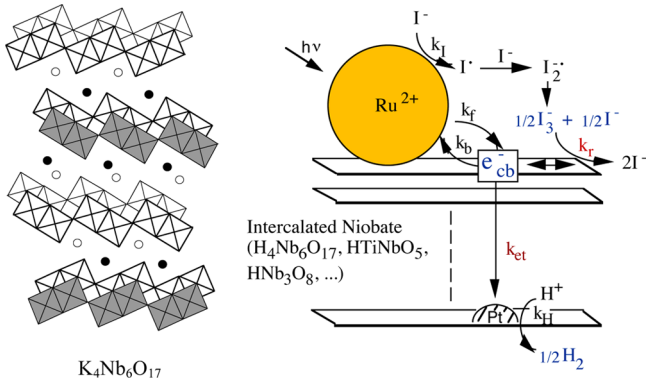

Figure 5. Scheme for visible-light H_2 evolution from aqueous solution containing I^-, a nonsacrificial electron donor. The idealized structure of $K_4Nb_6O_{17}$ is shown at the left. Reproduced from ref 5 with permission. Copyright 2009, American Chemical Society.

According to this concept, Matsumura et al. achieved simultaneous H_2 and O_2 evolution using a two-compartment photoelectrochemical cell, in which H_2 was evolved on Pt/rutile TiO_2 suspended in the cathode compartment using bromide as an electron donor, and O_2 evolution occurred on rutile TiO_2 dispersed in the anode compartment in the presence of Fe^{3+} as an electron donor.[31] A schematic illustration of this system is displayed in Figure 6. Reactions that occur on each photocatalyst are as follows:

$$2H^+ + 2e^- \rightarrow H_2 \quad (\text{on Pt/TiO}_2) \tag{7}$$

$$2Br^- + 2h^+ \rightarrow Br_2 \quad (\text{on Pt/TiO}_2) \tag{8}$$

$$Fe^{3+} + e^- \rightarrow Fe^{2+} \quad (\text{on TiO}_2) \tag{9}$$

$$2H_2O + 4h^+ \rightarrow O_2 + 4H^+ \quad (\text{on TiO}_2) \tag{10}$$

The oxidized product of bromine, Br_2, is spontaneously reduced on a Pt coil, while Fe^{2+} is oxidized to Fe^{3+} on the counterpart, according to the following equation, with a negative change in the Gibbs energy.

$$Br_2 + 2Fe^{2+} \rightarrow 2Br^- + 2Fe^{3+} \tag{11}$$

Thus, a water-splitting cycle could be made. However, this system did not produce H_2 and O_2 stoichiometrically as a result of the occurrence of some side reactions involving electron donor/acceptor pairs.

2.2. Metal Oxide Photocatalysts That Operate Z-Scheme Water Splitting into H_2 and O_2 with a Suitable Shuttle Redox Mediator.

2.2.1. Z-Scheme Water Splitting using Rutile TiO_2 or WO_3 As an O_2 Evolution Photocatalyst. According to the early works mentioned above, it is strongly suggested that suppressing the backward reactions involving redox reagents, which are thermodynamically downhill in most cases, while promoting forward reactions is the key to achieve water splitting into H_2 and O_2, according to the Z-scheme principle. Actually, successful Z-scheme water splitting systems, which will be discussed below, rely on photocatalytic materials that fit the bill.

The first demonstration of stoichiometric H_2 and O_2 evolution via Z-scheme water splitting was accomplished by Sayama et al. in 1997.[32] They coupled RuO_2-loaded WO_3, which operates water oxidation in the presence of Fe^{3+} ions, with a photochemical H_2 evolution system involving Fe^{2+} ions.

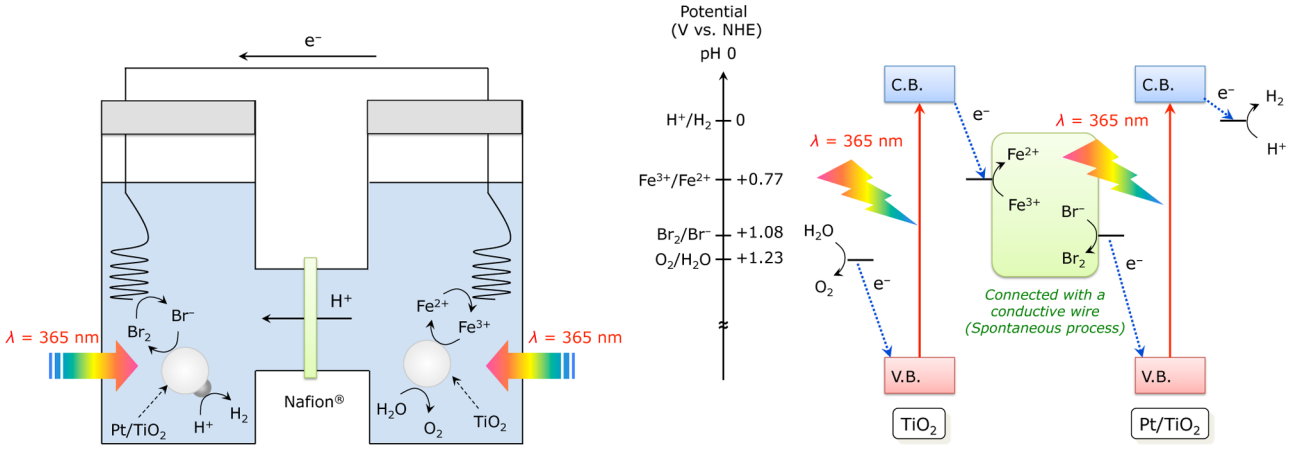

Figure 6. Schematic illustration of water-splitting cell using Pt/rutile TiO_2 and unmodified rutile TiO_2 in the presence of a Br_2/Br^- and Fe^{3+}/Fe^{2+} redox couple, respectively. Fe^{2+} ions produced as a result of photoreduction by TiO_2 react spontaneously with Br_2 that is the oxidation product by Pt/TiO_2, thereby regenerating Fe^{3+} and Br^- (see text for the detail). The energy diagram of this water-splitting cell is also depicted at the right.

dx.doi.org/10.1021/cs4002089 | ACS Catal. 2013, 3, 1486–1503

Under ultraviolet (UV) irradiation (λ > 200 nm), H_2 evolution occurs photochemically through excitation of Fe^{2+} by UV light, followed by photochemical reduction of water and the generation of Fe^{3+}, while the RuO_2/WO_3 photocatalyzes water oxidation using Fe^{3+} as an electron acceptor. It was also demonstrated that this system could produce H_2 and O_2 separately. As shown in Figure 7, only H_2 was evolved from an

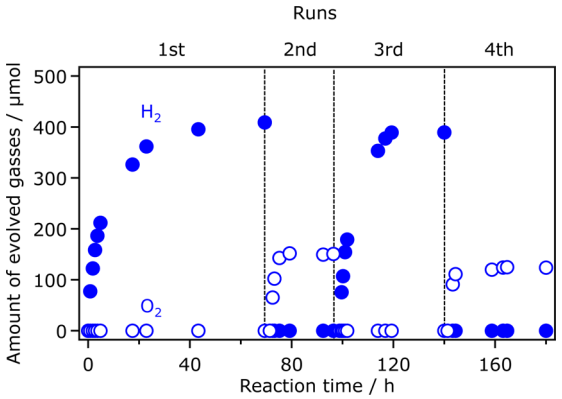

Figure 7. Separate evolution of H_2 and O_2 gases using a RuO_2/WO_3 catalyst and Fe^{3+}/Fe^{2+} redox system (H_2, solid circle; O_2, open circle). Run 1: Mixture of $FeSO_4$ (1 mmol) and H_2SO_4 (10 mmol) and distilled water (350 mL) was irradiated through a quartz glass filter (λ > 200 nm). Run 2: RuO_2 (1 wt %)/WO_3 catalyst (1 g) was added to the solution after run 1, and light was irradiated through a pyrex glass filter (λ > 300 nm). Run 3: Catalyst powder was filtered from the solution (or sedimented by stopping stirring) after run 2, and then the solution was irradiated again through a quartz glass filter (λ > 200 nm). Run 4: Same as run 2. Reproduced from ref 32 with permission. Copyright 1997, Elsevier B. V.

aqueous $FeSO_4$ solution without any photocatalyst powder under UV irradiation (λ > 200 nm), whereas only O_2 evolution occurred from the same reactant solution after addition of RuO_2/WO_3 powder under >300 nm irradiation.

In 2001, Abe and Sayama et al. succeeded in two-step water splitting using a system consisting of Pt/anatase TiO_2 and rutile TiO_2 as a H_2- and O_2-evolution photocatalyst, respectively, under UV irradiation (λ > 300 nm) in the presence of an IO_3^-/I^- redox mediator.[33] They also reported in the same year that visible-light water splitting (λ > 420 nm) was achieved using suspended particles of Pt-loaded $SrTiO_3$ doped with Cr and Ta (H_2 evolution photocatalyst, which was originally developed by Kudo et al.[34]) and PtO_x-loaded WO_3 (O_2 evolution photocatalyst) with an IO_3^-/I^- redox pair.[35,36] The optimized (Pt/$SrTiO_3$:Cr/Ta)−(PtO_x/WO_3) system gave an AQY of 1% at 420 nm.[37] The water-splitting reaction involving an IO_3^-/I^- redox couple was initiated by photooxidation of I^- into IO_3^- and photoreduction of H^+ into H_2 on a H_2 evolution photocatalyst, after which photoreduction of IO_3^- into I^- and photooxidation of H_2O into O_2 occurred on an O_2 evolution photocatalyst as follows:

$$I^- + 3H_2O + 6h^+ \rightarrow IO_3^- + 6H^+ \quad (12)$$

$$2H^+ + 2e^- \rightarrow H_2 \quad (13)$$

$$IO_3^- + 6e^- + 3H_2O \rightarrow I^- + 6OH^- \quad (14)$$

$$2H_2O + 4h^+ \rightarrow O_2 + 4H^+ \quad (15)$$

In these three Z-scheme systems mentioned above, the intrinsic properties of rutile TiO_2 and WO_3 allow for selective water oxidation. Because of their unique surface properties, water oxidation occurs on these photocatalysts even in the presence of electron donors such as Fe^{2+} and I^-, which are thermodynamically more susceptible to oxidation than water. Matsumura et al. have reported that photocatalytic oxidation of water on rutile TiO_2 powder proceeded efficiently with an AQY of ~9% at 365 nm when Fe^{3+} ions were used as an electron acceptor.[38] Their experiments revealed that Fe^{3+} ions are more susceptible to adsorption on rutile TiO_2 than Fe^{2+} ions, resulting in efficient water oxidation using Fe^{3+} as an electron acceptor, despite the fact that water oxidation is thermodynamically less favorable than oxidation of Fe^{2+} ions. Abe et al. measured the adsorption behavior of IO_3^- and I^- ions on a rutile TiO_2 powder.[37] As shown in Figure 8A, IO_3^- ions were easily adsorbed on the surface of rutile TiO_2, compared with I^- ions.

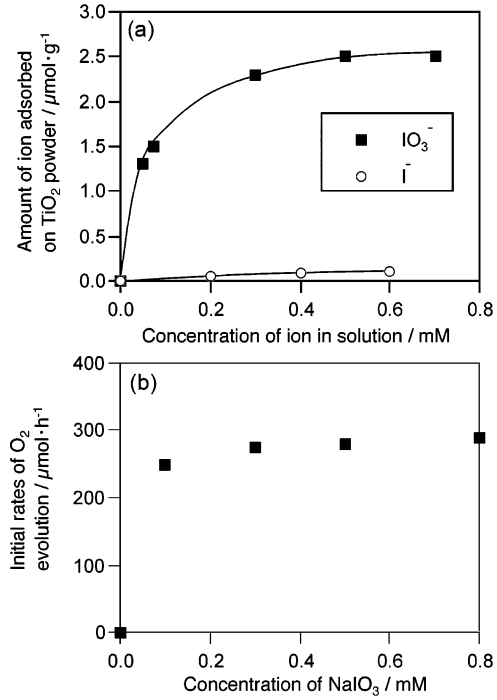

Figure 8. (a) Adsorption isotherms of IO_3^- and I^- anions on a rutile TiO_2 powder at 298 K. (b) Initial rates of O_2 evolution over the same rutile TiO_2 in the solutions (pH = 11) containing both 50 mM NaI and different concentrations of $NaIO_3$ under UV light irradiation (λ > 300 nm). Reproduced from ref 37 with permission. Copyright 2005, American Chemical Society.

Figure 8B shows the O_2 evolution rate over the rutile TiO_2 from an aqueous $NaIO_3$ solution with different concentrations. The rate of O_2 evolution was almost independent of the concentration of IO_3^- ions. A similar adsorption behavior of IO_3^- and I^- was observed in WO_3. Thus, the "selective water oxidation" on rutile TiO_2 and WO_3 appears to originate from their specific properties for adsorption of reactant ions. It should be also noted that the H_2 evolution rate from an aqueous NaI solution containing a H_2 evolution photocatalyst and either rutile TiO_2 or WO_3 in Z-scheme water splitting is much higher than that achieved using just a H_2 evolution photocatalyst. This is attributed to the high activity of these O_2 evolution photocatalysts for the reduction of IO_3^- ions, which

dx.doi.org/10.1021/cs4002089 | ACS Catal. 2013, 3, 1486−1503

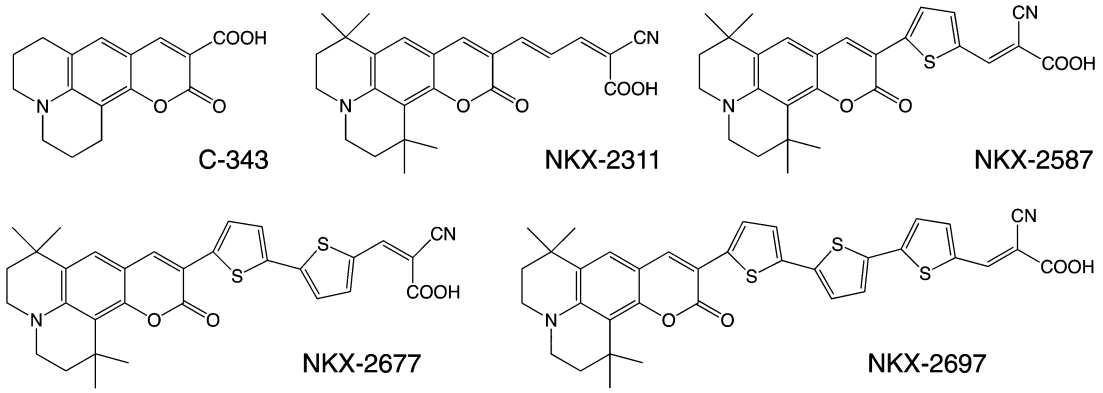

Figure 9. Structures of coumarin dyes employed as sensitizers for H_2 evolution. Reproduced from ref 10 with permission. Copyright 2011, The Chemical Society of Japan.

are generated as a result of oxidation of I^- by valence band holes in the H_2 evolution photocatalyst. The prompt reduction process would make the local concentration of IO_3^- around a H_2 evolution photocatalyst very low, thereby allowing for efficient water reduction.

In 2009, Abe et al. succeeded in splitting water into H_2 and O_2 using Pt-intercalated $H_2K_2Nb_6O_{17}$ sensitized by a coumarin dye for H_2 evolution, IrO_2−Pt-coloaded WO_3 for O_2 evolution, and an I_3^-/I^- redox couple under visible light ($\lambda > 410$ nm).[39] This system is similar to the HI photolysis system using $H_2K_2Nb_6O_{17}$ sensitized by a ruthenium complex, which was reported by Mallouk et al., as mentioned earlier.[27,28,30] The distinct difference is the sensitizers employed. Abe et al. examined various coumarin dyes as sensitizers, whose structures are shown in Figure 9. Steady H_2 evolution was observed when coumarin dyes having an oligothiophene moiety in their structure (NKX-2677 and NKX-2697) were employed, as shown in Figure 10a. In contrast, the H_2 evolution rate using

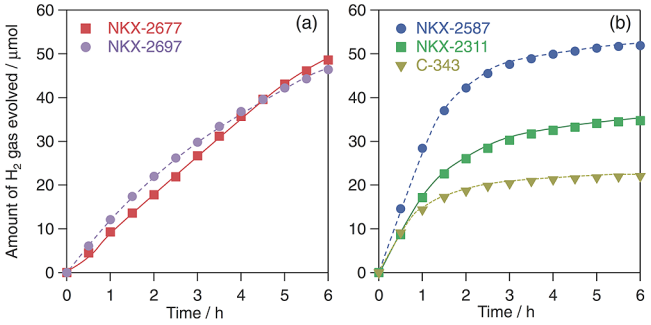

Figure 10. Time courses of photocatalytic H_2 evolution by coumarin dye-adsorbed Pt/$H_4Nb_6O_{17}$ photocatalysts (50 mg) suspended in a 0.1 M aqueous KI solution (100 mL) under visible light ($\lambda > 410$ nm). Reproduced from ref 10 with permission. Copyright 2011, The Chemical Society of Japan.

other coumarin dyes (C-343, NKX-2311, and NKX-2587) gradually decreased with irradiation time (Figure 10b). In Z-scheme water splitting, a similar result was observed. Electrochemical analysis showed that the oxidized states of coumarin dyes having an oligothiophene moiety in their structure are sufficiently kinetically stable, even in water, to allow for their regeneration by I^- ions. This robustness of the coumarin dye appears to contribute to the sustained H_2 evolution capability.

Sayama et al. recently reported that surface modification of WO_3 with Cs^+ ions was an effective means to improve the activity for photocatalytic O_2 evolution and Fe^{3+} reduction under visible light irradiation.[40] They claim that this modification involved the formation of ion-exchangeable sites on the WO_3 surface for H_3O^+ and Fe^{2+} ions, suitable for water oxidation and Fe^{3+} reduction, respectively. As a result, the Cs^+-modification resulted in a drastic increase in activity (~10 times), compared with unmodified WO_3. The optimized WO_3 showed an AQY of 19% at 420 nm and a solar-to-chemical energy conversion efficiency of 0.3%, although this photocatalytic system is not classified as Z-scheme water splitting.

Very recently, they conducted a similar Cs^+-treatment for PtO_x/WO_3 and succeeded in activating this material for O_2 evolution from an aqueous $NaIO_3$ solution with a maximum AQY of 20% at 420 nm.[41] It is noted that Cs^+-treated PtO_x/WO_3 exhibited water oxidation activity in the presence of I_3^- as an electron acceptor, but untreated analogue did not (as will be mentioned later[37]). This finding allowed one to perform Z-scheme water splitting in a wide pH range (pH 2−9) using a mixture of Pt/$SrTiO_3$:Cr/Ta and Cs^+-treated PtO_x/WO_3 under visible light, with an activity 3 times higher than that achieved using PtO_x/WO_3.

2.2.2. $BiVO_4$ as an O_2 Evolution Photocatalyst That Operates in the Presence of an Fe^{3+}/Fe^{2+} Redox Mediator. In 2004, Kudo et al. succeeded in extending the available wavelength for O_2 evolution up to 520 nm by employing $BiVO_4$.[42] $BiVO_4$ is a polymorphic compound, exhibiting tetragonal zircon, monoclinic scheelite, and tetragonal scheelite phases with different crystal structures.[43,44] Among these, the monoclinic scheelite phase having a band gap of 2.4 eV shows the highest performance as a photocatalyst for water oxidation using Ag^+ as an electron acceptor and exceeds the performance of WO_3, a representative photocatalyst for water oxidation.[45] Their Z-scheme system consisted of Pt-loaded $SrTiO_3$ doped with Rh (H_2 evolution photocatalyst)[46] and $BiVO_4$ (O_2 evolution photocatalyst), in which electron transport between the two photocatalysts was mediated by an Fe^{3+}/Fe^{2+} redox mediator.[42,47] They also conducted Z-scheme water splitting in a similar manner but with other O_2 evolution photocatalysts, such as Bi_2MoO_6 and WO_3. The results showed that there was no significant difference in activity among the three systems based on $BiVO_4$, Bi_2MoO_6 and WO_3 because the reactions on Pt/$SrTiO_3$:Rh limited the overall efficiency of the system. The AQYs of the these three systems, (Pt/$SrTiO_3$:Rh)−($BiVO_4$), −(Bi_2MoO_6), and −(WO_3), were 0.3, 0.2, and 0.2% at 440 nm, respectively. Figure 11 shows that the (Pt/$SrTiO_3$:Rh)−($BiVO_4$) system photocatalyzed water splitting under irradi-

dx.doi.org/10.1021/cs4002089 | ACS Catal. 2013, 3, 1486−1503

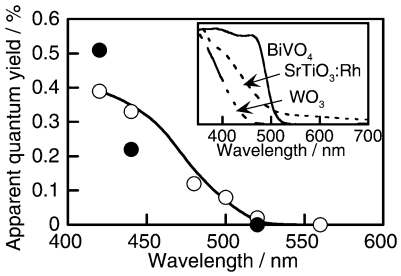

Figure 11. Photoresponse of the Z-scheme photocatalysis systems: $(Pt/SrTiO_3:Rh)-(BiVO_4)$, open marks; $(Pt/SrTiO_3:Rh)-(WO_3)$, closed marks. Catalyst, 20 mg for each component; reactant solution, 2 mM of aqueous $FeCl_3$ solution, 120 mL, pH 2.4; lamp, 300 W Xe arc lamp attached with optical filters to extract the monochromatic light from full arc; cell, top-irradiation cell with a Pyrex window. The inset shows diffuse reflection spectra of photocatalysts. Reproduced from ref 42 with permission. Copyright 2004, The Chemical Society of Japan.

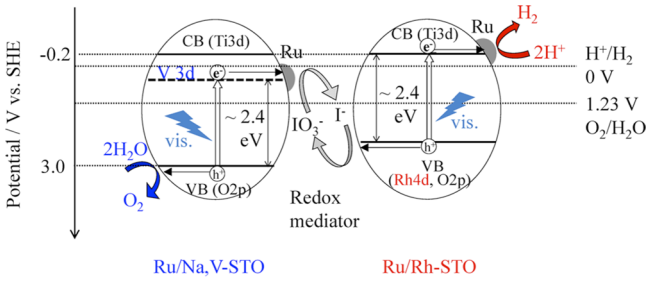

Figure 12. Schematic illustration of spontaneous H_2 and O_2 evolution by $Ru/SrTiO_3$:Na/V and $Ru/SrTiO_3$:Rh under irradiation with visible light in the presence of an IO_3^-/I^- redox mediator. Reproduced from ref 50 with permission. Copyright 2012, American Chemical Society.

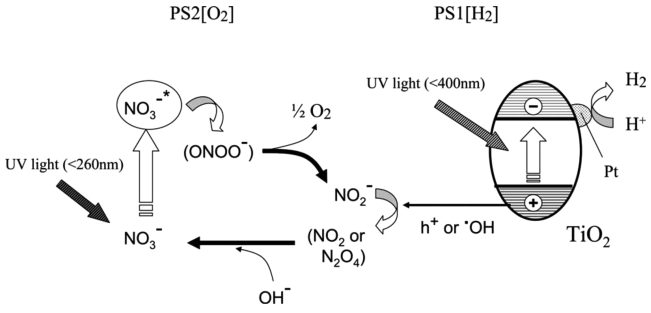

Figure 13. Proposed reaction mechanism for water splitting over Pt/TiO_2 suspended in aqueous $NaNO_2$. Reproduced from ref 51 with permission. Copyright 2006, Elsevier B. V.

ation with wavelength up to 520 nm, consistent with the absorption onsets of $SrTiO_3$:Rh and $BiVO_4$. On the other hand, the $(Pt/SrTiO_3:Rh)-(WO_3)$ system was active when it was irradiated with wavelength shorter than the absorption onset of WO_3. Kudo et al. also reported Z-scheme water splitting using $Ru/SrTiO_3$:Rh and $BiVO_4$ without redox mediators.[48] This system will be discussed in more detail later.

For application in a Z-scheme system based on an IO_3^-/I^- redox couple, however, $BiVO_4$ did not exhibit appreciable performance for water oxidation, primarily because of the competitive oxidation of I^- ions by valence band holes in the material.[37] Again, one can confirm the importance of O_2 evolution photocatalysts that do not show activity for backward reactions involving redox couples.

2.2.3. Z-Scheme Systems Consisting of Only Doped $SrTiO_3$ Photocatalysts with Controlled Band Structure. Very recently, Irie et al. reported Z-scheme water splitting systems using only $SrTiO_3$-based photocatalysts.[49,50] Among the materials they prepared, $SrTiO_3$:Ga/Bi and $SrTiO_3$:In/V were able to reduce and oxidize water to form H_2 and O_2, respectively, in the presence of an IO_3^-/I^- redox couple, achieving Z-scheme water splitting under UV irradiation (λ < 400 nm). The dopants of Bi and V in each $SrTiO_3$ photocatalyst form a new valence and conduction band in the forbidden band of $SrTiO_3$, thereby allowing for visible light absorption, although unfortunately, this system did not work under only visible light (λ > 400 nm).

They also developed a similar Z-scheme water splitting system consisting of doped $SrTiO_3$ photocatalysts that worked under visible light (λ > 420 nm). Na- and V-codoped $SrTiO_3$, modified with Ru cocatalyst, achieved the functionality as an O_2 evolution photocatalyst in Z-scheme water splitting in the presence of an IO_3^-/I^- redox couple, when it was combined with $Ru/SrTiO_3$:Rh H_2 evolution photocatalyst, which was originally developed by Kudo et al.[46] A schematic illustration of this reaction system is depicted in Figure 12.

2.2.4. NO_3^-/NO_2^- Redox Systems. In addition to Fe^{3+}/Fe^{2+} and IO_3^-/I^- couples, Sayama et al. reported another Z-scheme water splitting system in which Pt-loaded TiO_2 anatase worked as a H_2 evolution photocatalyst and a NO_3^-/NO_2^- couple serves as a redox mediator,[51] and O_2 evolution occurred via direct photoexcitation of NO_3^-, followed by decomposition. As schematically illustrated in Figure 13, the reaction was conducted in an aqueous $NaNO_2$ solution under UV irradiation (λ > 200 nm) that is able to photoexcite NO_3^- ions. Pt/TiO_2 produces H_2 using NO_2^- ions as electron donors. Under irradiation of light with wavelength shorter than 260 nm, the oxidation product (NO_3^-) undergoes photoexcitation to give NO_3^-* species, which are photodecomposed into NO_2^- and O_2 via some intermediates, such as peroxynitrus acid ($ONOO^-$). Thus, stoichiometric water splitting into H_2 and O_2 is achieved.

Both the activity and stability were improved by the addition of Na_2CO_3 to the $NaNO_2$ solution, and stoichiometric decomposition of water into H_2 and O_2 took place for a long time (>5 days). It is also noted that water splitting using other photocatalysts, such as $Pt/SrTiO_3$ and $Pt/K_4Nb_6O_{17}$, was achievable in a similar manner in the presence of $NaNO_2$ and Na_2CO_3, although the detailed effects of Na_2CO_3 with $NaNO_2$ on Z-scheme water splitting have not fully been clarified.

2.2.5. Co^{3+}/Co^{2+} Redox Systems. Very recently, Kudo et al. reported that $[Co(bpy)_3]^{3+/2+}$ and $[Co(phen)_3]^{3+/2+}$ (bpy = 2,2′-bipyridine; phen = 1,10-phenanthroline) redox couples achieved the functionality to mediate electron transfer from $BiVO_4$ to $Ru/SrTiO_3$:Rh, resulting in stable overall water splitting, with a maximum AQY of 2.1% at 420 nm.[52] Although $SrTiO_3$:Rh modified with Pt or Ru was active for H_2 evolution half reaction under visible light (λ > 420 nm) using $[Co(bpy)_3]^{2+}$ or $[Co(phen)_3]^{2+}$ as an electron donor, Pt/anatase TiO_2 and $Pt/SrTiO_3$ exhibited little activity under band gap irradiation (λ > 300 nm). These results suggest that the doped Rh species in $SrTiO_3$ not only contribute to visible-light response, but also host active sites for the oxidation of $[Co(bpy)_3]^{2+}$ and $[Co(phen)_3]^{2+}$ ions. Interestingly, the reduction of $[Co(bpy)_3]^{3+}$ or $[Co(phen)_3]^{3+}$ by photogenerated electrons in the $SrTiO_3$:Rh catalysts, which is a backward reaction, was very slow.

dx.doi.org/10.1021/cs4002089 | ACS Catal. 2013, 3, 1486−1503

In contrast, O_2 evolution from an aqueous solution containing $[Co(bpy)_3]^{3+}$ or $[Co(phen)_3]^{3+}$ as an electron acceptor over $BiVO_4$ was markedly suppressed in the presence of $[Co(bpy)_3]^{2+}$or $[Co(phen)_3]^{2+}$, indicating that the oxidation of these divalent complexes by photogenerated holes in the valence band of $BiVO_4$ competed with water oxidation. They noted that applying other photocatalysts either to H_2 or O_2 evolution system (e.g., undoped $SrTiO_3$ and anatase TiO_2 for H_2 evolution; Cr/Sb-codoped rutile TiO_2 and WO_3 for O_2 evolution) in the presence of these Co^{3+}/Co^{2+} pairs resulted in low activity. As mentioned above, holes generated in the donor level of $SrTiO_3$:Rh would be able to oxidize Co^{2+} species, thereby giving the corresponding oxidation product of Co^{3+}, whereas the lack of such active oxidation sites in other photocatalysts is expected to contribute to poorer activity. The difference in O_2 evolution, on the other hand, could be explained in terms of the oxidation power of each photocatalyst: namely, Cr/Sb-codoped rutile TiO_2 and WO_3, which possess relatively high oxidation power due to the deeper valence band formed by O2p orbitals than the Bi6s,6p valence band maximum in $BiVO_4$, promote oxidative decomposition of the cobalt complexes rather than just extracting one electron. It was also demonstrated that using a membrane filter to isolate each photocatalyst suspension in a reaction cell, H_2 and O_2 were separately produced, although the H_2/O_2 ratio evolved was not exactly stoichiometric.

2.3. (Oxy)nitride Based Z-Scheme Systems with an IO_3^-/I^- Redox Mediator. Many efforts have thus been made to construct Z-scheme water splitting systems using metal oxides. Until around 2005, actually, Z-scheme water splitting under visible light was achieved using several combinations of a H_2 evolution photocatalyst (e.g., doped $SrTiO_3$) and an O_2 evolution photocatalyst (e.g., WO_3 and $BiVO_4$).[35−37,41,42,47,48,52] However, using a doped material appears to be somewhat disadvantageous for the development of an efficient Z-scheme water splitting system. The doped elements not only form a donor or acceptor level in the forbidden band of the material as a center for absorption at visible wavelengths, but also obstruct the rapid migration of photogenerated electrons or holes at the surface and in the material bulk, since the dopant frequently provides a discrete energy level rather than an energy band.[4] Actually, the bottleneck process in Z-scheme water splitting consisting of a doped $SrTiO_3$ (e.g., $SrTiO_3$:Cr/Ta and $SrTiO_3$:Rh) has been reported to be the H_2 evolution process.[37,42] A new photocatalyst that is capable of producing H_2 in a Z-scheme system was thus highly desirable.

Compared with metal oxide photocatalysts, (oxy)nitrides (although they have been originally developed as visible-light-driven photocatalysts for one-step water splitting) may be more interesting compounds for application in Z-scheme water splitting because of their light-harvesting property and band-edge positions suitable for both water reduction and oxidation.[2] Figure 14 shows the schematic band structures of a metal oxide ($NaTaO_3$) and oxynitride ($BaTaO_2N$), both of which have the same perovskite structure. The top of the valence band for the metal oxide consists of O 2p orbitals. When N atoms are partially or fully substituted for O atoms in a metal oxide, the valence band maximum of the material is expected to shift higher compared with the corresponding metal oxide owing to N 2p orbitals having a higher potential energy than the O 2p orbital, without affecting the conduction band minimum. This has been confirmed by density functional theory (DFT) calculations. As a result, most (oxy)nitrides have band gaps sufficiently small to respond to visible light (<3 eV). In this section, Z-scheme water splitting systems consisting of (oxy)nitrides are reviewed. UV−visible diffuse reflectance spectra of oxynitride materials discussed below are shown in Figure 15. (Oxy)nitrides can be readily obtained by heating a corresponding metal oxide powder under a flow of ammonia gas at high temperature (typically 1123−1273 K).[2]

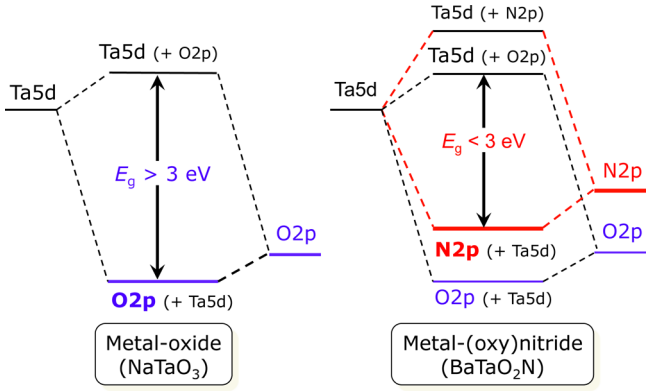

Figure 14. Schematic band structures of a metal oxide ($NaTaO_3$) and metal oxynitride ($BaTaO_2N$) with perovskite structure. Reproduced from ref 2 with permission. Copyright 2007, American Chemical Society.

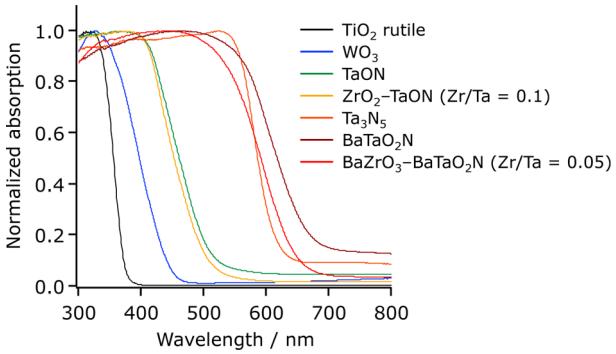

Figure 15. UV−visible diffuse reflectance spectra for some (oxy)-nitrides that have been applied to Z-scheme water splitting.

2.3.1. TaON. TaON is a photocatalyst that is capable of reducing and oxidizing water individually to form H_2 and O_2 in the presence of suitable electron donors and acceptors, respectively, under band gap irradiation (λ < 520 nm).[53] In 2005, Abe et al. applied Pt-loaded TaON as a H_2 evolution photocatalyst to a Z water-splitting system.[54] Pt/TaON produced H_2 from an aqueous solution containing NaI as an electron donor under visible light, although the rate of H_2 evolution decreased with reaction time. This deactivation is ascribed to the backward reaction (photoreduction of IO_3^- by photogenerated electrons), which takes place in the conduction band of the catalyst, as observed in other H_2 evolution photocatalysts.[35−37] Note that neither O_2 nor N_2 was produced during the reaction, indicating that photogenerated holes in the valence band of TaON efficiently oxidize I^- into IO_3^-, which is consistent with the results of photoelectrochemical analyses for TaON electrode.[55] The combination of Pt/TaON and PtO_x/WO_3 with an IO_3^-/I^- redox mediator resulted in stoichiometric water splitting into H_2 and O_2 under visible light, with an AQY

dx.doi.org/10.1021/cs4002089 | ACS Catal. 2013, 3, 1486−1503

of 0.5% at 420 nm. The water-splitting behavior was stable at pH 5.3, producing stoichiometric H_2 and O_2 during 60 h of reaction.[56] With suitable modification by cocatalysts, TaON also functioned as a building block for O_2 evolution in Z-scheme water splitting in the presence of an IO_3^-/I^- redox couple,[57,58] as will be discussed in the latter section.

2.3.2. $ATaO_2N$ (A = Ca, Sr, and Ba). For more efficient utilization of visible light in H_2 evolution, perovskite oxynitrides of $ATaO_2N$ (A = Ca, Sr, Ba) having absorption edges at 520, 600, and 660 nm (see Figure 15), respectively, were examined as a H_2 evolution photocatalyst for Z-scheme water splitting.[59] Modification of these perovskite oxynitrides with Pt as a water reduction promoter resulted in observable H_2 evolution from an aqueous NaI solution under visible light. However, Sr-analogue produced not only H_2 but also N_2 as a result of self-oxidative decomposition of the material. Z-scheme water splitting into H_2 and O_2 proceeded photocatalytically when $Pt/CaTaO_2N$ or $Pt/BaTaO_2N$ was employed as a building block for H_2 evolution in combination with PtO_x/WO_3 as an O_2 evolution photocatalyst and an IO_3^-/I^- redox couple. The AQY for the $BaTaO_2N$-based system was ~0.1% at 420−440 nm. Although the available wavelength of light for H_2 evolution in the Z-scheme water splitting system was extended to 660 nm by employing $BaTaO_2N$, the water splitting rate gradually decreased over time, with the ratio of H_2/O_2 evolved being deviated from stoichiometry. It is claimed that the deactivation is attributable to an accumulation of I_3^- in the reactant solution after the extended reaction.[60] Since I_3^- does not work as an efficient electron acceptor as IO_3^- for PtO_x/WO_3 because of its poorer adsorption characteristics of I_3^-, photogenerated electrons in the conduction band of PtO_x/WO_3 are unable to reduce I_3^- effectively, contributing to inefficient O_2 evolution.

2.3.3. Activation of Oxynitrides for Enhanced H_2 Evolution by Surface Modification. Surface modification is sometimes done in an attempt to improve the quality of the photocatalyst surface. Because the surface of a photocatalyst hosts active sites for redox reactions and is where charge transport occurs, modification of the surface to bring about a desired property or specific function is important.[8] The most commonly known method is to load a cocatalyst that promotes surface redox reactions, as will be introduced in the latter section. In this section, surface modification techniques that improve photocatalytic activity toward Z-scheme water splitting are reviewed.

As mentioned earlier, TaON works as a building block for H_2 evolution in a Z-scheme water splitting system in the presence of an IO_3^-/I^- redox mediator.[54,56] However, it was suggested that the TaON component limited the overall efficiency of this Z-scheme system. According to the results of photoelectrochemical analyses on TaON electrodes, which showed that the oxidation of I^- ions by valence band holes in TaON efficiently occurs,[55] one can presume that the water reduction process is the rate-determining step. Because TaON is an intermediate phase between Ta_2O_5 and Ta_3N_5, it seems difficult to control the crystallinity of TaON by adjustment of the preparation parameters alone. Furthermore, because of its low thermal stability, postcalcination to reduce the density of defects appears to be disadvantageous for TaON. In fact, postcalcination of TaON under O_2 or N_2 was found to result in a decrease in activity.[61]

To overcome such issues in the synthesis of TaON, a new strategy to reduce surface defects on TaON was developed using ZrO_2 as a "protector" through a surface modification technique.[62] As has been observed for other tantalum-based (oxy)nitrides such as Ta_3N_5[63] and $CaTaO_2N$,[64] the reduction of Ta^{5+} cations in TaON during nitridation generates reduced tantalum species (e.g., Ta^{3+} or Ta^{4+}), resulting in the production of anionic vacancies to keep the charge balance of the material. The thus-formed defect sites can act as recombination centers between photogenerated electrons and holes. On the other hand, when ZrO_2, more resistant to thermal ammonolysis than Ta_2O_5, is loaded on the surface of Ta_2O_5, Ta^{5+} cations at the interface between Ta_2O_5 (and/or TaON) and the loaded ZrO_2 are expected to interact with ZrO_2 and thereby become more cationic. As a result, it is expected that the undesirable reduction of Ta^{5+} cations during nitridation would be suppressed. The above-mentioned idea and the preparation scheme are shown in Figure 16.

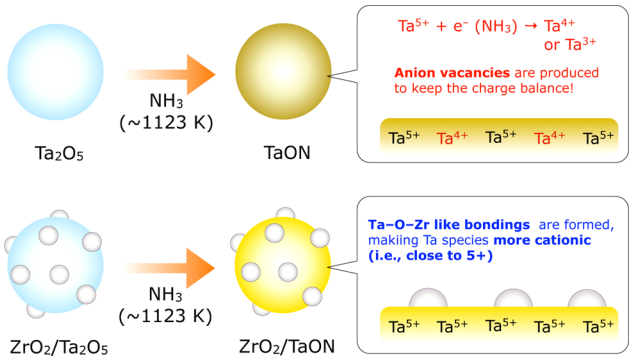

Figure 16. Nitridation of the ZrO_2/Ta_2O_5 composite to produce ZrO_2/TaON while suppressing the production of reduced tantalum species (defect sites) near the surface of the material. Reproduced from ref 13 with permission from the PCCP Owner Societies.

It was found that the as-prepared ZrO_2-modified TaON (represented as ZrO_2/TaON) exhibited enhanced water reduction behavior compared with unmodified TaON. In particular, combining Pt-loaded ZrO_2/TaON with PtO_x/WO_3 and an IO_3^-/I^- shuttle redox mediator achieved stoichiometric water splitting into H_2 and O_2 under visible light, yielding an AQY of 6.3% under irradiation by 420 nm monochromatic light under optimal conditions, six times greater than the yield achieved using a TaON analogue.[65] To the best of the author's knowledge, this is the highest reported value to date for a nonsacrificial, visible-light-driven water-splitting system. This enhancement of activity was considered to be attributed to the reduced density of defects in ZrO_2/TaON, which contributes to a lower probability of undesirable electron−hole recombination in ZrO_2/TaON than in TaON. Follow-up study on this system revealed that a lower density of anionic defects in TaON, which was realized using highly dispersed ZrO_2 nanoparticles (10−30 nm in size), contributed primarily to the enhanced H_2 evolution activity.[66]

Activation of $BaTaO_2N$ was also attempted by employing Zr(IV) modification in a similar manner to ZrO_2/TaON to reduce the density of anionic defects during nitridation from Ba−Ta oxide precursor to $BaTaO_2N$.[67] Althuogh a composite of $BaZrO_3$ and $BaTaO_2N$ was supposed to be obtained according to the initial expectation, however, the nitrided product of $BaZrO_x$-modified $BaTaO_x$ (Zr/Ta molar ratio ≤0.1) was not a composite of $BaZrO_3$ and $BaTaO_2N$ but a solid solution of the two. According to a report by Grins and Svensson, who prepared $BaZrO_3$−$BaTaO_2N$ solid solutions (with some byproduction of Ta_3N_5) by nitriding sol−gel-

dx.doi.org/10.1021/cs4002089 | ACS Catal. 2013, 3, 1486−1503

derived Ba−Zr−Ta oxides, the lattice mismatch between $BaZrO_3$ and $BaTaO_2N$ is ∼2%, and hence, they can form solid solutions over the entire range of substitution.[68]

Nevertheless, the $BaZrO_3$−$BaTaO_2N$ solid solution exhibited an activity for H_2 evolution from an aqueous NaI solution, a half reaction of Z-scheme water splitting, 6−9 times higher than unmodified $BaTaO_2N$. For Z-scheme water splitting in combination with PtO_x/WO_3 and an IO_3^-/I^- redox couple, an AQY of ∼0.6% at 420−440 nm was obtained. This value was at least 6 times greater than that previously obtained using $BaTaO_2N$. Compared with $BaTaO_2N$, the $BaZrO_3$−$BaTaO_2N$ solid solutions had at least two positive characteristics as a photocatalyst: an enlarged band gap and a reduced defect density, as indicated by UV−visible diffuse reflectance spectra. The former should enhance reduction and oxidation capability, owing to the increased driving force for all chemical reactions. The latter should lower the probability of electron−hole recombination, which is most undesirable in photocatalysis. The enhanced photocatalytic activity of the $BaZrO_3$−$BaTaO_2N$ solid solution is considered to be the result of these two beneficial properties. However, a gradual decrease in the crystallinity of $BaZrO_3$−$BaTaO_2N$ was observed when the $BaZrO_3$ content was increased. The decrease in crystallinity would contribute to an activity drop that occurred at the Zr/Ta ratio ranging from 0.05 to 0.1. A schematic illustration of the band structures of $BaZrO_3$−$BaTaO_2N$ solid solution and the end compounds is displayed in Figure 17. Stoichiometric water splitting under simulated sunlight (air-mass 1.5 irradiation) was also achieved using the optimized $BaZrO_3$−$BaTaO_2N$ solid solution as a H_2 evolution photocatalyst, in combination with either PtO_x/WO_3 or rutile TiO_2.[69] Interestingly, the Pt/$BaZrO_3$−$BaTaO_2N$ + PtO_x/WO_3 system produced H_2 and O_2 simultaneously in the presence of an Fe^{3+}/Fe^{2+} redox couple, being different from other reported oxynitrides, although the performance was much lower than that recorded with an IO_3^-/I^- redox couple.

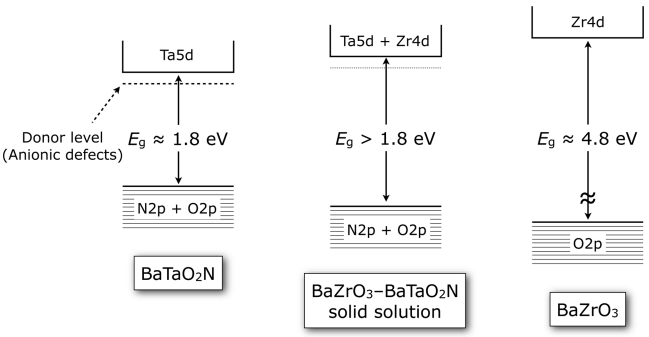

Figure 17. Schematic illustration of band structures of $BaZrO_3$−$BaTaO_2N$ solid solution and the end compounds. Reproduced from ref 13 with permission from the PCCP Owner Societies.

2.3.4. Surface Modification of Ta_3N_5 with Rutile TiO_2 Nanoparticles for Application in Oxygen Evolution. For Z-scheme water splitting in the presence of a given redox couple, controlling the adsorption of redox species onto the photocatalyst is of particular importance to facilitate the desirable forward reaction(s) and suppress the undesirable side reaction(s), as discussed in section 2.2.1. and depicted in Figure 2. Ohno et al. demonstrated that visible-light-driven water oxidation on WO_3 in an aqueous solution containing Fe^{3+} as an electron acceptor can be improved by coating WO_3 particles with a thin TiO_2 layer.[70] It was shown that the TiO_2 layer provided adsorption sites for Fe^{3+} rather than Fe^{2+}, allowing one to form O_2 more efficiently in the presence of Fe^{2+} ions, which competed with water oxidation.

Similarly, Domen et al. recently applied rutile TiO_2 nanoparticles as a modifier on Ta_3N_5 having a 600 nm absorption edge to achieve functionality as an O_2 evolution photocatalyst in a two-step water splitting system with an IO_3^-/I^- shuttle redox mediator under visible light (λ > 420 nm) in combination with a Pt/ZrO_2/TaON H_2 evolution photocatalyst.[71] The rutile TiO_2 modifier suppressed the adsorption of I^- on Ta_3N_5, allowing Ta_3N_5 to evolve O_2 in a two-step water-splitting system, with further modification by Ir nanoparticles that functioned as reduction sites for IO_3^- ions. Thus, it became possible to utilize visible light up to 600 nm (corresponding to the absorption edge of Ta_3N_5) for an O_2 evolution system in Z-scheme water splitting.

Although the role of the loaded Ir will be discussed in the latter section, here, the effect of rutile TiO_2 as a modifier is presented. Figure 18 compares the rate of O_2 evolution from an aqueous $NaIO_3$ solution containing NaI on modified Ta_3N_5 photocatalysts under visible light with a schematic illustration of the structure of this material, which was revealed by physicochemical analyses. The O_2 evolution activity of Ir/rutile TiO_2/Ta_3N_5 in an aqueous solution containing both IO_3^- and I^- was 10 times higher than that of Ir/Ta_3N_5. In this

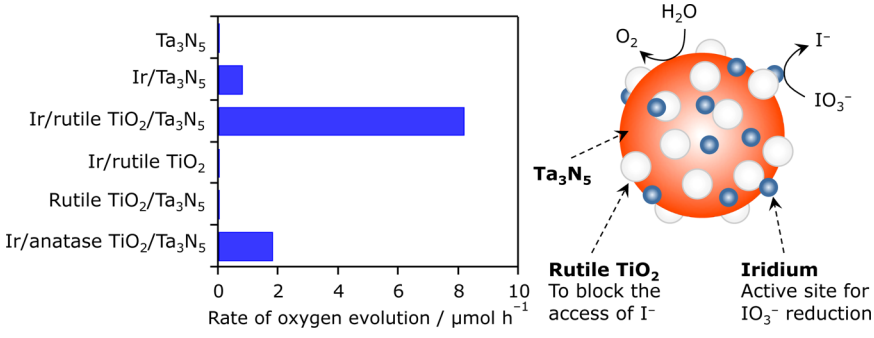

Figure 18. Initial rate of O_2 evolution on modified Ta_3N_5 photocatalysts from an aqueous $NaIO_3$ solution (4 mM) containing NaI (1 mM) under visible light (λ > 420 nm). A schematic illustration of the most active Ir/TiO_2 rutile/Ta_3N_5 photocatalyst is also depicted. Reaction conditions: catalyst, 0.05 g; aqueous solution, 250 mL; light source, xenon lamp (300 W) fitted with a cutoff filter; reaction vessel, Pyrex side-irradiation type. Reproduced from ref 71 with permission. Copyright 2010, American Chemical Society.

dx.doi.org/10.1021/cs4002089 | ACS Catal. 2013, 3, 1486−1503

enhancement, rutile TiO_2 worked not as a photocatalyst but as a modifier, because Ir-loaded rutile TiO_2, without Ta_3N_5, did not evolve O_2 from an aqueous $NaIO_3$ solution, even without NaI under visible light ($\lambda > 420$ nm). In addition, rutile TiO_2/Ta_3N_5 without Ir cocatalyst showed no O_2 evolution activity in the same condition, indicating that the TiO_2 rutile did not function as a cocatalyst to promote the surface reaction. It is also interesting to note that a similarly prepared sample, Ir/anatase TiO_2/Ta_3N_5, did not work as effectively as Ir/rutile TiO_2/Ta_3N_5. According to the previous report, anatase TiO_2 does not have the aforementioned unique adsorption property observed in rutile TiO_2.[37] This result further supports the idea that the relatively high activity of Ir/rutile TiO_2/Ta_3N_5 is attributed to the rutile TiO_2 modifier on Ta_3N_5, which hinders the access of I^- anions.

3. EFFECTS OF REDOX MEDIATORS ON ACTIVITY OF Z-SCHEME WATER SPLITTING

Although there are some exceptions, a shuttle redox mediator is, in principle, an essential component to driving Z-scheme water splitting by two different photocatalysts because it plays a role of transferring electrons from an O_2 evolution photocatalyst to a H_2 evolution photocatalyst. Therefore, the character of a shuttle redox mediator has a significant impact on the efficiency of a given Z-scheme water splitting system. In addition, there are some direct interactions between redox mediators and the surface of cocatalysts, thereby affecting activity. The most employed redox couples are Fe^{3+}/Fe^{2+} and IO_3^-/I^-, both of which have unique characters affecting the efficiency of Z-scheme water splitting, as will be discussed below.

3.1. Dependence of Activity on the Concentration of a Redox Mediator. Taking an IO_3^-/I^- couple for example, Z-scheme water splitting is usually initiated using not iodate salt (e.g., $NaIO_3$) but iodide salt (e.g., NaI), primarily because H_2 evolution reaction is significantly suppressed in the presence of IO_3^- ions that is more susceptible to reduction than protons. With increasing the concentration of NaI, the efficiency of the I^- oxidation by valence band holes in a H_2 evolution photocatalyst is enhanced, resulting in improved water reduction to give more H_2. On the other hand, the forward oxidation reaction in the O_2 evolution side (that is, water oxidation) is suppressed as a result of competitive oxidation of I^- by holes photogenerated in the valence band of the O_2 evolution photocatalyst. Accordingly, as shown in Figure 19,

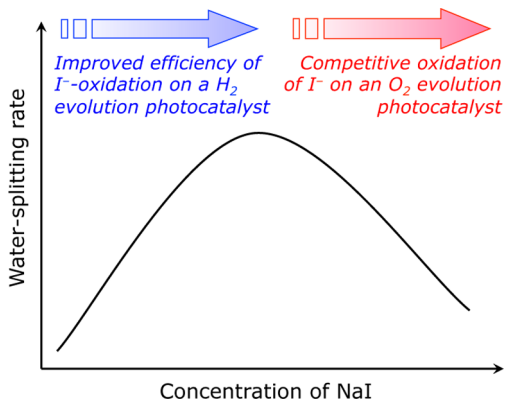

Figure 19. Trade-off between the concentration of a reducing reagent (e.g., NaI) and water-splitting rate.

there is a volcano-type trend between the concentration of NaI and Z-scheme activity in most cases (as observed in several Z-scheme systems[37,56,65]). In the case of an Fe^{3+}/Fe^{2+} couple, the situation seems to be similar to IO_3^-/I^--based systems, although, to the author's knowledge, the effect of the Fe^{3+}/Fe^{2+} concentration on Z-scheme water splitting (neither its half reactions nor a Z-scheme system involving direct photoexciation of Fe^{2+}) has yet to be reported.

3.2. Reaction pH. The pH of the reactant solution affects the efficiency of Z-scheme water splitting. The available reaction pH in an Fe^{3+}/Fe^{2+} redox system is limited to the acidic condition because iron ions undergo precipitation to give iron hydroxide in neutral and basic conditions. On the other hand, it is possible to perform a reaction in a wide range of pH when an IO_3^-/I^- couple is employed. In this section, therefore, the effects of reaction pH on activity of Z-scheme water splitting are discussed, with a focus on IO_3^-/I^- systems.

It is generally known that products generated as a result of photooxidation of I^- ions are strongly dependent on the reaction pH. In addition to reaction 12, there is another reaction path for the oxidation of I^- by valence band holes in a photocatalyst, as follows:[37]

$$3I^- + 2h^+ \rightarrow I_3^- \quad (16)$$

I_3^- produced by eq 16 does not act as an effective electron acceptor for O_2 evolution by many photocatalysts, including rutile TiO_2 and PtO_x/WO_3; therefore, a higher pH is preferable for reaction 12 to proceed. However, I_3^- ions are also converted into I^- and IO_3^- via the following disproportional reaction:[72]

$$3I_3^- + 3H_2O \rightarrow 8I^- + IO_3^- + 6H^+ \quad (17)$$

This reaction proceeds more smoothly in basic reaction conditions than in acidic conditions. Consequently, in most cases involving an IO_3^-/I^- couple, the rates of H_2 and O_2 evolution increase with an increase in the pH to reach a maximum at a certain point. In addition to this pH-dependent character of the IO_3^-/I^- redox couple, changing the reaction pH of course affects the base photocatalyst, as exemplified by photocatalytic water splitting systems driven by one-step photoexcitation.[8] For example, WO_3 has inherent instability in a basic solution (pH > 7) and, hence, work more efficiently at pH below 7.[37]

Figure 20 shows an example of pH-dependent Z-scheme water splitting activity in 0.1 M NaI solution using Pt/anatase TiO_2 and rutile TiO_2 as a H_2 and O_2 evolution photocatalyst, respectively.[37] Negligible O_2 evolution was observed at pH 3 because the O_2 evolution photocatalyst, rutile TiO_2, is unable to reduce I_3^-, which was the main oxidation product on Pt/anatase TiO_2. In the pH range of 5−7, O_2 evolution was observable, but the ratio of H_2/O_2 did not meet the stoichiometry because of the accumulation of I_3^- in the reactant solution. The accumulation of I_3^- ions might also cause another undesirable impact on activity by absorbing incident photons around 350 nm. In basic conditions above pH 9, both H_2 and O_2 were evolved stoichiometrically, and the gas evolution rates were much higher than those in acidic conditions, indicating that a basic condition is more desirable for efficient water splitting.

3.4. Redox Mediator-Free Z-Scheme System. It was thus shown that redox mediators are, in principle, indispensable and play vital roles in achieving Z-scheme water splitting, but can cause several kinds of undesirable backward reactions.

dx.doi.org/10.1021/cs4002089 | ACS Catal. 2013, 3, 1486−1503

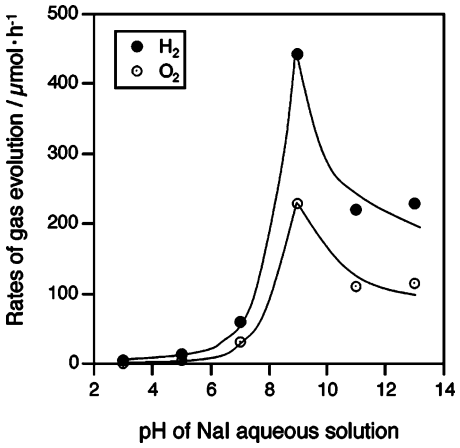

Figure 20. Dependence of rates of gas evolution over a mixture of Pt-loaded anatase TiO_2 and rutile TiO_2 photocatalysts upon the pH value of NaI solution (NaI = 0.1 M). Reproduced from ref 37 with permission. Copyright 2005, American Chemical Society.

Hence, a Z-scheme water splitting system that does not rely on any redox mediator is highly desirable. This idea of a redox mediator-free system may seem a photocatalytic material that has a built-in electric field between the interface of p- and n-type semiconductor.[73,74]

In 2009, Kudo et al. reported a unique Z-scheme water splitting system consisting of $Ru/SrTiO_3$:Rh as a H_2 evolution photocatalyst and a wide variety of O_2 evolution photocatalysts (such as TiO_2:Cr/Sb, $BiVO_4$ and WO_3).[48] This system was capable of stoichiometrically splitting water into H_2 and O_2 under visible light without a redox mediator. The activity was strongly dependent on the reaction pH, and the highest activity was obtained at pH 3.5, where powders of $Ru/SrTiO_3$:Rh and $BiVO_4$ aggregated together. On the basis of the results of photoluminescence measurements and photocatalytic reactions, it was concluded that electrons transfer from the conduction band of an O_2 evolution photocatalyst to an impurity level formed by reversible Rh species (namely, Rh^{4+}/Rh^{3+}) in the forbidden band of $SrTiO_3$, thereby achieving stable water splitting by two-step photoexcitation according to Z-scheme, with an AQY of 1.7% at 420 nm and a solar-to-hydrogen energy conversion efficiency of 0.12%. The reaction scheme of this system is schematically illustrated in Figure 21. Their study also suggested that the interparticle electron transfer process is the rate-determining step and that the activity will be improved by realizing more intimate contact between each photocatalyst. Ta_3N_5 modified with CoO_x and Ir was also applicable as an O_2 evolution photocatalyst to this redox mediator-free Z-scheme system.[75]

Very recently, reduced graphene oxide (GO) was found to function as a solid-state electron mediator for Z-scheme water splitting consisting of $Ru/SrTiO_3$:Rh and $BiVO_4$, contributing to an enhanced activity.[76] It is claimed that achieving the best balance between the extent of GO reduction and the hydrophobicity is a crucial factor in determining how efficiently GO works as an electron mediator in this Z-scheme photocatalytic water splitting system. In this particular case, photocatalytically reduced GO by $BiVO_4$ had high electron conductivity and a low degree of hydrophobicity, which led to the enhanced Z-scheme activity.

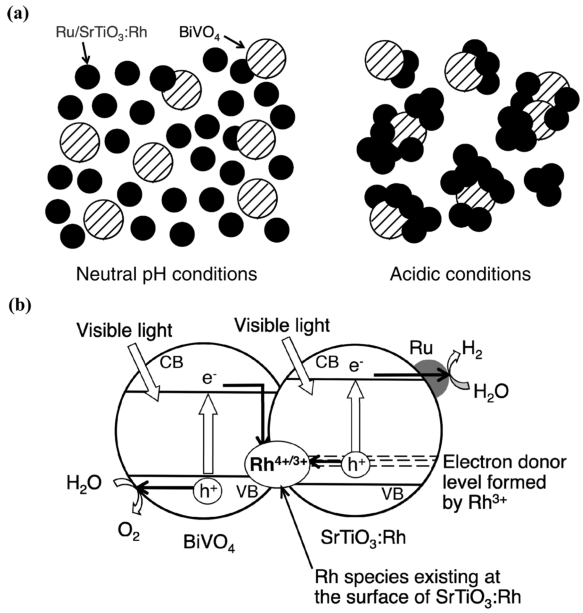

Figure 21. Mechanism of water splitting using the Z-scheme photocatalysis system driven by electron transfer between H_2- and O_2-evolution photocatalysts. (a) Suspension of $Ru/SrTiO_3$:Rh and $BiVO_4$ at neutral and acidic conditions. (b) Scheme of photocatalytic water splitting. Reproduced from ref 48 with permission. Copyright 2009, American Chemical Society.

4. ROLES OF COCATALYSTS IN Z-SCHEME WATER SPLITTING

4.1. Improved Selectivity for Water Oxidation Catalysis on TaON by Loading Bifunctional RuO_2 Cocatalyst. A number of semiconductor materials have thus been applied to Z-scheme water splitting, aimed especially at extending the available wavelength for the water splitting reaction to utilize more visible light. In addition to efficient utilization of visible light, it is important to control the selectivity of chemical reactions that occur during Z-scheme water splitting. As shown in Figure 2, the reduction of A and oxidation of D are, respectively, more likely to occur on H_2 and O_2 evolution photocatalysts, compared with water reduction and oxidation. For this reason, the number of Z-scheme water splitting systems showing a reasonable level of activity under visible light is limited as discussed earlier, even though a large number of visible-light-responsive photocatalysts that are capable of reducing or oxidizing water have been developed.[4] Thus, controlling the selectivity for the forward reactions on each photocatalyst is important from the standpoint of establishing a highly efficient Z-scheme system.

It has been reported that the intrinsic properties of a photocatalyst allow for selective water reduction and oxidation. Taking O_2 evolution photocatalysts, for example, rutile TiO_2 and WO_3 were presented as such "selective" photocatalysts for water oxidation, as discussed earlier. Owing to their unique surface properties, water oxidation occurs on these photocatalysts even in the presence of electron donors such as Fe^{2+} and I^-, which are thermodynamically more susceptible to oxidation than water. The origin of this unique surface property of rutile TiO_2 and WO_3 has not been clarified completely. Nevertheless, there are some reports that suggest a surface-dependent preferential water oxidation ability of rutile TiO_2. For example, Nakato et al. have proposed that the (100) crystal face of rutile TiO_2 has a favorable property for water

dx.doi.org/10.1021/cs4002089 | ACS Catal. 2013, 3, 1486−1503

oxidation.[77] Ohno et al. have suggested that the crystal face of anatase and rutile TiO_2 play a role in facilitating electron−hole separation, resulting in different reactivities.[78]

It is also possible to achieve such selective catalysis by the introduction of a proper nanoparticulate cocatalyst on the photocatalyst surface.[8] RuO_2-loaded TaON is such an example. This material is an effective photocatalyst for O_2 evolution to achieve Z-scheme overall water splitting in combining with Pt-loaded TaON as a H_2 evolution photocatalyst using an IO_3^-/I^- shuttle redox mediator.[57] This is the first example of a two-step water splitting system that consists solely of a nonoxide-type compound. TaON alone was not applicable to an O_2 evolution system in the presence of an IO_3^-/I^- pair, most likely because the competitive oxidation of I^- occurred efficiently, as mentioned earlier. On the other hand, loading RuO_2 on TaON enabled water oxidation even in the presence of I^-.

This unique behavior of RuO_2 loaded on TaON was investigated with respect to the preparation condition.[58] The structure of nanoparticulate Ru species dispersed on TaON as cocatalysts was also characterized in more detail by means of X-ray absorption spectroscopy and scanning electron microscopy. Using $(NH_4)_2RuCl_6$ as the precursor, RuO_2 nanoparticles with an optimal distribution, as determined by the preparation conditions, were demonstrated to act as a bifunctional cocatalyst for TaON to promote the reduction of IO_3^- and the oxidation of water. However, experimental results also suggested that the efficiency of this system is limited by the competitive oxidation of I^- with the valence band holes in RuO_2/TaON and the photoreduction of O_2 that can occur on the RuO_2/TaON surface. A schematic illustration of the mechanism of Z-scheme water splitting using Pt/TaON and RuO_2/TaON is depicted in Figure 22. Similar to a Z-scheme

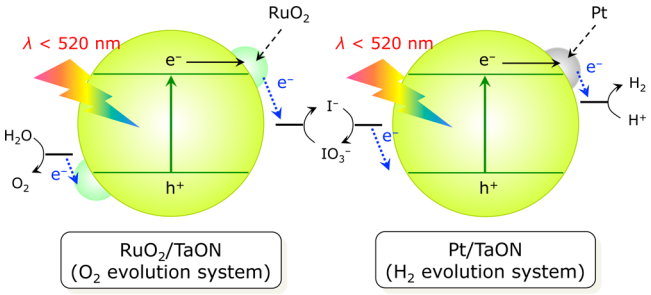

Figure 22. A schematic illustration of Z-scheme water splitting using Pt/TaON and RuO_2/TaON in the presence of an IO_3^-/I^- redox mediator.

water splitting system consisting of Pt/TaON and PtO_x/WO_3, the activity of this TaON-based Z-scheme system was significantly enhanced by simply replacing Pt/TaON with Pt/ZrO_2/TaON.[13]

4.2. Cocatalyst as Active Sites for Multielectron Reduction. In addition to the functionality to achieve selective catalysis, the fundamental roles of cocatalysts loaded on a photocatalyst are to extract charge carriers from the photocatalyst and to offer active sites for redox reactions.[6,8] In particular, cocatalysts that can offer an electron sink to promote multielectron reduction are necessary to drive Z-scheme water splitting. First, without exception, loading a cocatalyst that can promote water reduction (a 2-electron process) was found to be indispensable in all cases of reported Z-scheme systems. The most suitable cocatalyst to drive water reduction appears to depend on electron donors used. As exemplified by ZrO_2/TaON that was employed as a H_2 evolution photocatalyst in combination with PtO_x/WO_3 O_2 evolution photocatalyst in the presence of an IO_3^-/I^- redox couple, loading Pt cocatalyst on ZrO_2/TaON gave the highest activity for Z-scheme water splitting among the cocatalysts examined,[65] although the distinct reason has not been fully understood. Although Ru-loaded ZrO_2/TaON exhibited much higher activity than Pt-loaded analogue from an aqueous methanol solution,[62,66] the former was less active for H_2 evolution in an IO_3^-/I^--mediated Z-scheme water splitting system. It should be also noted that the size of Pt cocatalyst has a significant impact on activity. In a Z-scheme water splitting system consisting of Pt/ZrO_2/TaON as a H_2 evolution photocatalyst, it was revealed that a more uniform dispersion and smaller Pt cocatalyst nanoparticles on the ZrO_2/TaON surface contributed primarily to improved performance.[65]

In Z-scheme systems with an IO_3^-/I^- redox couple, a cocatalyst that can facilitate the reduction of IO_3^- ions (a 6-electron process) appears to be necessary to allow for efficient water oxidation, except for rutile TiO_2, which does not require any cocatalyst to produce O_2 from an aqueous $NaIO_3$ solution.[37] For example, although unmodified WO_3 exhibits little activity for the reaction, modification of WO_3 with nanoparticulate PtO_x as a cocatalyst results in observable O_2 evolution.[56,79] Electrochemical measurements using porous WO_3 electrodes suggested that the loaded PtO_x cocatalyst collected photogenerated electrons, reducing IO_3^- into I^-.[79] In RuO_2/TaON that was introduced in the previous section (4.1), it is likely that facilitating the reduction of IO_3^- is the key to drive water oxidation in an aqueous $NaIO_3$ solution because modification of TaON with IrO_2, which is known as one of the most active water oxidation promoters, did not lead to O_2 evolution under identical reaction conditions.[57]

Ir-loaded Ta_3N_5 is another interesting example that allows one to achieve O_2 evolution from an aqueous solution containing IO_3^- ions under visible light, as mentioned in the previous section (2.3.4). To clarify the function of the loaded Ir cocatalyst, electrochemical measurements were conducted using porous Ta_3N_5 electrodes in an aqueous solution containing IO_3^- ions.[71] The results indicated that the reduction of IO_3^- on the surface of Ta_3N_5 was very slow, because little current was observed in the unmodified Ta_3N_5 electrode (Figure 23b). However, an appreciable cathodic current was observed in an Ir-modified Ta_3N_5 electrode, and this current was markedly increased by the addition of IO_3^- ions to the

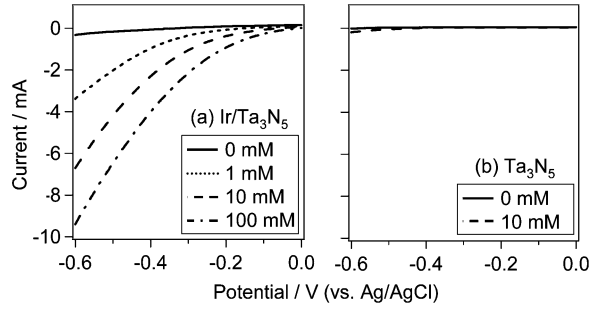

Figure 23. Current−voltage curves of Ta_3N_5 electrodes (a) with and (b) without loading Ir in an aqueous Na_2SO_4 solution (0.1 M) containing different concentrations of $NaIO_3$. Reproduced from ref 71 with permission. Copyright 2010, American Chemical Society.

dx.doi.org/10.1021/cs4002089 | ACS Catal. 2013, 3, 1486−1503

solution (Figure 23a). The Ir cocatalyst loaded on Ta_3N_5 greatly assisted the reduction of IO_3^-, probably by functioning as an active site for the reduction reaction. Moreover, although bare Ta_3N_5 photocatalyst did not show H_2 evolution activity from an aqueous solution containing methanol as an electron donor, Ir/Ta_3N_5 photocatalyst did. On the basis of these results, it was concluded that Ir on Ta_3N_5 functions as a cocatalyst that can promote the multielectron reduction reaction.

4.3. Effect of Shuttle Redox Mediators on Cocatalysts. In addition to the role of shuttling electrons, redox mediators play another hidden role(s) in Z-scheme water splitting. It is noted that in most cases, nanoparticulate Pt cocatalysts loaded on a photocatalyst catalyze water formation from H_2 and O_2, a thermodynamically downhill reaction, thereby lowering the water-splitting rate.[80,81] As a result, Pt-loaded semiconductor photocatalysts do not work efficiently in pure water. Z-scheme water-splitting systems consisting of an IO_3^-/I^- redox couple discussed earlier, however, do generate H_2 and O_2 stoichiometrically even in the presence of Pt cocatalyst (see Table 1). Abe et al. have claimed that I^- ions undergo preferential adsorption onto the surface of Pt, spontaneously forming an iodine layer, which effectively suppressed the backward reaction of water formation.[82]

Somewhat similar to the behavior of iodine species on Pt, unique behavior of an Fe^{3+}/Fe^{2+} redox mediator has been reported by Kato et al.[47] They examined the effects of an Fe^{3+}/Fe^{2+} redox couple on the activity of Z-scheme water splitting using $Pt/SrTiO_3$:Rh (H_2 evolution photocatalyst) and $BiVO_4$ (O_2 evolution photocatalyst). In that study, it was found that Fe^{2+} existing in the reactant solution suppressed water oxidation on $BiVO_4$ but water reduction on $Pt/SrTiO_3$:Rh was enhanced in the presence of Fe^{3+} ions with concentration higher than Fe^{2+}. They attributed the enhanced activity for water reduction to the suppression of backward reaction that can occur on the surface of the loaded Pt; that is, H_2-O_2 recombination (water formation), and the reduction of Fe^{3+} on the Pt surface, both of which are efficiently suppressed by adsorption of $[Fe(SO_4)(H_2O)_5]^+$ and/or $[Fe(OH)(H_2O)_5]^{2+}$ on the Pt surface. This situation is schematically illustrated in Figure 24.

Although the backward reaction of water formation on Pt was not completely suppressed by adsorbed iron species,[47] further studies revealed that Ru was able to become an alternative cocatalyst that does not suffer from the water formation, even without lowering the forward reaction rate in a Z-scheme system consisting of $SrTiO_3$:Rh as a H_2 evolution photocatalyst.[83] Other backward reactions, the reduction of Fe^{3+} by H_2 and oxidation of Fe^{2+} by O_2, were also suppressed by simply replacing Pt with Ru on $SrTiO_3$:Rh, resulting in stable water splitting even in an extended period of reaction, as shown in Figure 25.

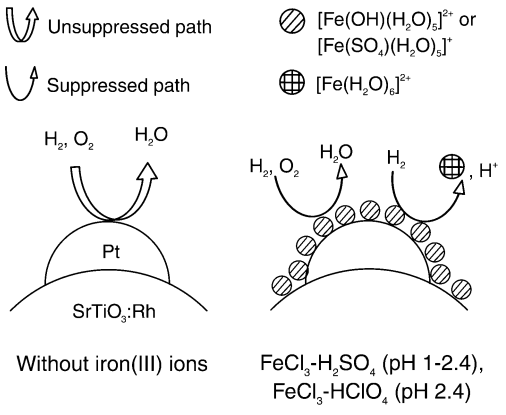

Figure 24. Suppression of backward reactions by iron(III) ions in Z-scheme water splitting using $Pt/SrTiO_3$:Rh and $BiVO_4$. Reproduced from ref 47 with permission. Copyright 2007, The Chemical Society of Japan.

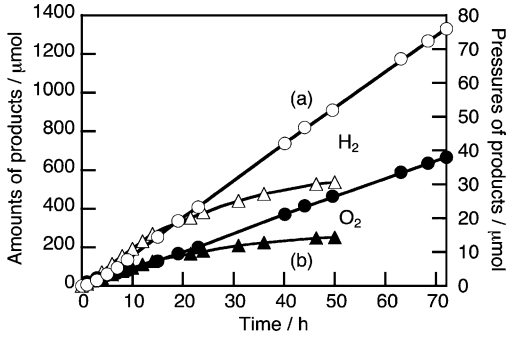

Figure 25. Photocatalytic overall water splitting on (a) the (Ru (0.7 wt %)/$SrTiO_3$:Rh)−($BiVO_4$) system and (b) the (Pt (0.1 wt %)/$SrTiO_3$:Rh)−($BiVO_4$) system. Catalyst, 50 mg each; reactant solution, 2 mM of aqueous $FeCl_3$ solution, 120 mL, pH 2.4; light source, 300 W Xe arc lamp ($\lambda > 420$ nm); cell, top-irradiation cell with a Pyrex glass window. Reproduced from ref 83 with permission. Copyright 2008, Elsevier B. V.

It can thus be concluded that in most cases, a redox mediator is indispensable not only to realizing electron transfer between different photocatalyst particles but also to suppressing backward reactions. Adjusting the optimal concentration of a redox mediator, which, of course, depends on each Z-scheme system constructed, maximizes the water-splitting rate in Z-scheme.

5. OTHER Z-SCHEME SYSTEMS

In this last section, powder-based photochemical systems, claimed to work according to Z-scheme principle, for reactions other than water splitting into H_2 and O_2 are briefly reviewed.

5.1. Solid-State Z-Scheme Systems. With a focus on site-selective coupling of different materials to create a highly efficient photocatalytic system, Tada et al. developed an anisotropic $CdS/Au/TiO_2$ nanojunction, in which CdS (reduction site), TiO_2 (oxidation site) and the interconnect Au are spatially fixed.[84] This three-component system exhibited higher photocatalytic activity for the reduction of methylviologen (MV^+) than the single- and two-component systems did. The enhanced activity was claimed to be vectorial electron transfer driven by the two-step excitation of TiO_2 and CdS, similar to Z-scheme. The proposed energy diagram is shown in Figure 26.

Liu et al. reported a composite of ZnO and CdS that generated H_2 from an aqueous solution containing SO_3^{2-} and S^{2-} ions as electron donors.[85] The rate of H_2 evolution by the composite material, dependent on the ZnO/CdS ratio, was faster than that recorded using either ZnO or CdS alone. Liu et al. concluded that upon band gap excitation of the two semiconductors, electron transfer took place from the conduction band of ZnO to the valence band of CdS, as observed in the lifetime of photoluminescence, and that the Z-

dx.doi.org/10.1021/cs4002089 | ACS Catal. 2013, 3, 1486−1503

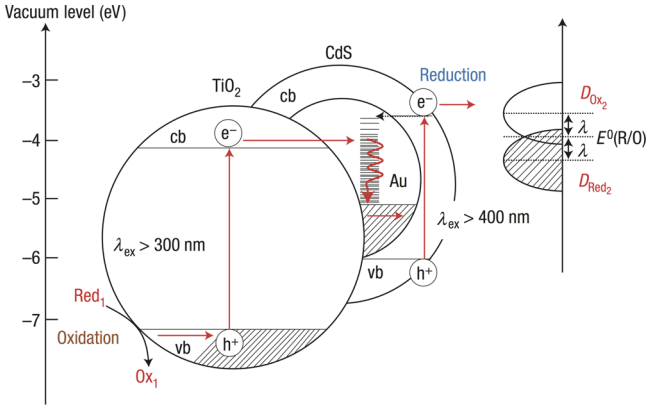

Figure 26. Energy band diagram scheme of the CdS−Au−TiO_2 system. E^0(R/O) is the standard electrode potential of MV^+/MV^{2+}. D_{Red2} and D_{Ox2} represent the distribution function for occupied and unoccupied states, respectively, and λ is the reorganization energy. Reproduced from ref 84 with permission. Copyright 2006, Nature Publishing Group.

scheme-like electron transfer contributed to the enhanced performance. Very recently, the activity of this system was found to be further enhanced by placing a Au interconnect between ZnO and CdS due to improved electron transfer from ZnO to CdS mediated by Au.[86]

A similar system consisting of TiO_2 and heteropoly blue driven by UV (λ < 365 nm) and visible (λ < 675 nm) photons, respectively, was reported to exhibit an enhanced activity for H_2 evolution from a water−glycerol mixture, compared with either TiO_2 or heteropoly blue.[87] It was suggested that the improvement of activity achieved by the composite material was ascribed to electron transfer from TiO_2 to heteropoly blue according to Z-scheme.

5.2. Plasmonic Systems. Recently, photocatalytic reactions driven by localized surface plasmonic resonance (LSPR) have attracted attention.[88−92] For application in Z-scheme-like photoreactions, some research papers have been published.

Yu et al. developed $H_2WO_4{\cdot}H_2O$/Ag/AgCl composite nanoplates, which exhibited higher photocatalytic activity for the degradation of methyl orange in the presence of molecular O_2 than similarly prepared analogues consisting of one or two of the three components.[93] They claimed that two-step visible-light absorption was caused by the LSPR of metallic Ag nanoparticles and the band gap photoexcitation of $H_2WO_4{\cdot}H_2O$, leading to the improved photocatalytic activity.

Zan et al. prepared a three-component composite photocatalyst of Ag/AgX/BiOX (X = Cl, Br).[94] The Ag/AgX/BiOX composites showed enhanced photocatalytic activity for the degradation of rhodamine B under visible light, which was higher than Ag/AgX and BiOX. In this system, Ag was suggested to play a different role in photocatalytic reactions, depending on X: SPR for Ag/AgCl/BiOCl (X = Cl), and a Z-scheme bridge for Ag/AgBr/BiOBr (X = Br).

5.3. Semiconductor/Metal-Complex Hybrid Photocatalyst for Z-Scheme CO_2 Reduction. Photocatalytic CO_2 reduction is another important reaction in the research of artificial photosynthesis.[95] Very recently, Ishitani et al. developed a new type of Z-scheme system for photocatalytic CO_2 reduction using Ag-loaded TaON semiconductor and a Ru(II) dinuclear complex.[96] This Z-scheme system was capable of converting visible-light energy into chemical energy in the form of formic acid and formaldehyde, with a positive change in the Gibbs energy of 83.0 kJ mol^{-1}. Isotope experiments indicated that this hybrid material photocatalytically produced formic acid as the major reduction product and formaldehyde as the oxidation product from CO_2 and methanol, respectively. Under visible light (λ > 400 nm), both Ag/TaON and the sensitizer unit in the supramolecular complex undergo photoexcitation. The conduction band electrons in Ag/TaON migrate to the excited state or oxidized sensitizer unit, producing a one-electron reduced species. Subsequent intermolecular electron transfer occurs from the one-electron-reduced species in the photosensitizer unit to the catalyst unit, as it is a thermodynamically downhill process. Finally, holes left in the valence band of Ag/TaON oxidize methanol to give formaldehyde, whereas electrons transferred to the catalyst unit reduce CO_2 into formic acid. Since the CO_2 reduction to give formic acid is a two-electron process, the stepwise two-photon absorption and the subsequent electron transfer events are likely to occur twice during the reaction to give one HCOOH molecule. The reaction scheme is displayed in Figure 27.

6. SUMMARY AND OUTLOOK

The research on Z-scheme water splitting using two different photocatalysts and a shuttle redox mediator was reviewed, with a focus on the historical development of new photocatalysts as well as the roles of redox mediators and cocatalysts that

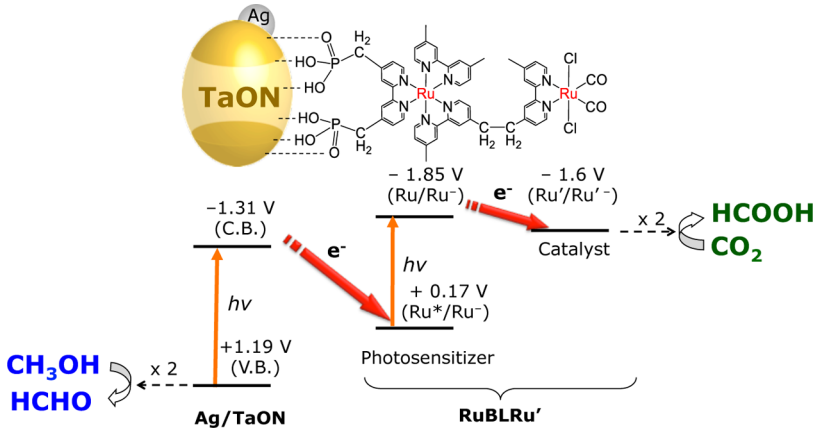

Figure 27. Artificial Z-scheme for photocatalytic CO_2 reduction using Ag-loaded TaON semiconductor and a Ru(II) dinuclear complex (RuBLRu'). Reproduced from ref 96 with permission. Copyright 2013, American Chemical Society.

dx.doi.org/10.1021/cs4002089 | ACS Catal. 2013, 3, 1486−1503

promote surface chemical reactions on a photocatalyst. Although more than 30 years have passed since the Z-scheme research was triggered, it was about a decade ago that visible-light-driven Z-scheme water splitting was accomplished. The key to achieving the reaction was the finding that certain metal oxide photocatalysts are capable of selectively oxidizing water even in the presence of electron donors such as Fe^{2+} and I^-. Another effective way to control the selectivity for the forward reactions is to modify a photocatalyst with a nanoparticulate cocatalyst, as exemplified by RuO_2/TaON. Although water splitting by visible light had once been described as one of the "Holey Grails" of chemistry,[24] it became possible for one to achieve the reaction with visible light around 400−500 nm using certain Z-scheme systems, with AQYs of ∼6%.

Because the water reduction process is the rate-determining step for Z-scheme water splitting in most cases, improving the H_2 evolution system is a straightforward way to further enhance activity of known systems. Taking WO_3-based photocatalysts for example, AQYs of 10−20% at 420 nm for O_2 evolution half reaction in the presence of either IO_3^- or Fe^{3+} have already been attained.[40,41,79] These AQY values for O_2 evolution are much higher than those achieved in Z-scheme water splitting with suitable H_2 evolution photocatalysts. It means that there still remains significant room for improvement in H_2 evolution systems toward highly efficient Z-scheme water splitting. As discussed before, suppressing backward reactions involving shuttle redox mediators appears to be one of the biggest challenges in the development of efficient Z-scheme water splitting systems. In this regard, redox mediator-free Z-scheme systems may be the ultimate solution, although how efficiently back electron transfer, which is thermodynamically downhill, between two different semiconductors takes place remains unknown. It is also important to explore new cocatalysts that efficiently promote forward reactions but do not exhibit activity for the backward reactions (of course, including H_2−O_2 recombination).

The development of a photocatalyst that operates under a wide range of visible light is another important subject in Z-scheme research from the viewpoint of efficient solar energy conversion. Assuming overall water splitting with an AQY of unity, the theoretical potential of photocatalysts with a 500 nm absorption edge is 7.9% solar-energy-conversion efficiency, and photocatalysts with an absorption edge of 600 and 650 nm can achieve 16.2 and 20.6% conversion, respectively.[6] At present, the absorption wavelengths available for H_2 and O_2 evolution have been increased to 660 nm (using $BaTaO_2N$ and its variant) and 600 nm (using Ta_3N_5), respectively; however, there still remains a challenge in coupling these "600 nm-class" photocatalysts to construct a Z-scheme water splitting that works under irradiation with wavelength longer than 600 nm.

A tentative goal for research on H_2 production via solar-driven overall water splitting using a particulate photocatalyst is to develop a stable photocatalytic system that can achieve an AQY of 30% at 600 nm.[2] The state of the art in Z-scheme water splitting is far below the target, as discussed above. Therefore, more-efficient Z-scheme systems that can operate under a wide range of visible light must be developed.

AUTHOR INFORMATION

Corresponding Author

*Phone: +81-3-5734-2239. Fax: +81-3-5734-2284. E-mail: maedak@chem.titech.ac.jp.

Notes

The authors declare no competing financial interest.

ACKNOWLEDGMENTS

The author thanks a PRESTO/JST program and a Grant-in-Aid for Young Scientists (Start-up) (No. 21850009) from the Japan Society for the Promotion of Science (JSPS) for their funding support. Acknowledgement is also extended to Nippon Sheet Glass Foundation for Materials Science and Engineering.

REFERENCES

(1) Lee, J. S. *Catal. Surv. Asia* **2005**, *9*, 217.
(2) Maeda, K.; Domen, K. *J. Phys. Chem. C* **2007**, *111*, 7851.
(3) Inoue, Y. *Energy Environ. Sci.* **2009**, *2*, 364.
(4) Kudo, A.; Miseki, Y. *Chem. Soc. Rev.* **2009**, *38*, 253.
(5) Youngblood, W. J.; Lee, S.-H. A.; Maeda, K.; Mallouk, T. E. *Acc. Chem. Res.* **2009**, *42*, 1966.
(6) Maeda, K.; Domen, K. *J. Phys. Chem. Lett.* **2010**, *1*, 2655.
(7) Chen, X.; Shen, S.; Guo, L.; Mao, S. S. *Chem. Rev.* **2010**, *110*, 6503.
(8) Maeda, K. *J. Photochem. Photobiol., C* **2011**, *12*, 237.
(9) Kudo, A. *MRS Bull.* **2011**, *36*, 32.
(10) Abe, R. *Bull. Chem. Soc. Jpn.* **2011**, *84*, 1000.
(11) Wang, Y.; Wang, X.; Antonietti, M. *Angew. Chem., Int. Ed.* **2012**, *51*, 68.
(12) Osterloh, F. E. *Chem. Soc. Rev.* **2013**, *42*, 2294.
(13) Maeda, K. *Phys. Chem. Chem. Phys.* **2013**, in press; DOI: 10.1039/C2CP43914J.
(14) Fujishima, A.; Honda, K. *Nature* **1972**, *238*, 37.
(15) Domen, K.; Naito, S.; Soma, M.; Onishi, T.; Tamaru, K. *J. Chem. Soc., Chem. Commun.* **1980**, 543.
(16) Lehn, J. M.; Sauvage, J. P.; Ziessel, R. *Nouv. J. Chim.* **1980**, *4*, 623.
(17) Sato, S.; White, J. M. *Chem. Phys. Lett.* **1980**, *72*, 83.
(18) Scaife, D. E. *Sol. Energy* **1980**, *25*, 41.
(19) Williams, R. *J. Chem. Phys.* **1960**, *32*, 1505.
(20) Ellis, A. B.; Kaiser, S. W.; Bolts, J. M.; Wrighton, M. S. *J. Am. Chem. Soc.* **1977**, *99*, 2839.
(21) Krasnovskii, A. A.; Brin, G. P. *Dokl. Akad. Nauk. SSSR* **1962**, *147*, 656.
(22) Darwent, J. R.; Mills, A. *J. Chem. Soc., Faraday Trans. 2* **1982**, *78*, 359.
(23) Erbs, W.; Desilvestro, J.; Borgarello, E.; Grätzel, M. *J. Phys. Chem.* **1984**, *88*, 4001.
(24) Bard, A. J.; Fox, M. A. *Acc. Chem. Res.* **1995**, *28*, 141.
(25) Bard, A. J. *J. Photochem.* **1979**, *10*, 59.
(26) Krishnan, C. V.; Brunschwig, B. S.; Creutz, C.; Sutin, N. *J. Am. Chem. Soc.* **1985**, *107*, 2005.
(27) Kim, Y. I.; Salim, S.; Huq, M. J.; Mallouk, T. E. *J. Am. Chem. Soc.* **1991**, *113*, 9561.
(28) Kim, Y. I.; Atherton, S. J.; Brigham, E. S.; Mallouk, T. E. *J. Phys. Chem.* **1993**, *97*, 11802.
(29) Ohno, T.; Saito, S.; Fujihara, K.; Matsumura, M. *Bull. Chem. Soc. Jpn.* **1996**, *69*, 3059.
(30) Saupe, G. B.; Mallouk, T. E.; Kim, W.; Schmehl, R. H. *J. Phys. Chem. B* **1997**, *101*, 2508.
(31) Fujihara, K.; Ohno, T.; Matsumura, M. *J. Chem. Soc., Faraday Trans.* **1998**, *94*, 3705.
(32) Sayama, K.; Yoshida, R.; Kusama, H.; Okabe, K.; Abe, Y.; Arakawa, H. *Chem. Phys. Lett.* **1997**, *277*, 387.
(33) Abe, R.; Sayama, K.; Domen, K.; Arakawa, H. *Chem. Phys. Lett.* **2001**, *344*, 339.
(34) Ishii, T.; Kato, H.; Kudo, A. *J. Photochem. Photobiol., A* **2004**, *163*, 181.
(35) Sayama, K.; Mukasa, K.; Abe, R.; Abe, Y.; Arakawa, H. *Chem. Commun.* **2001**, 2416.
(36) Sayama, K.; Mukasa, K.; Abe, R.; Abe, Y.; Arakawa, H. *J. Photochem. Photobiol., A* **2002**, *148*, 71.

(37) Abe, R.; Sayama, K.; Sugihara, H. *J. Phys. Chem. B* **2005**, *109*, 16052.
(38) Ohno, T.; Haga, D.; Fujihara, K.; Kaizaki, K.; Matsumura, M. *J. Phys. Chem. B* **1997**, *101*, 6415.
(39) Abe, R.; Shinmei, K.; Hara, K.; Ohtani, B. *Chem. Commun.* **2009**, 3577.
(40) Miseki, Y.; Kusama, H.; Sugihara, H.; Sayama, K. *J. Phys. Chem. Lett.* **2010**, *1*, 1196.
(41) Miseki, Y.; Fujiyoshi, S.; Gunji, T.; Sayama, K. *Catal. Sci. Technol.* **2013**, in press. DOI: 10.1039/c3cy00055a.
(42) Kato, H.; Hori, M.; Konta, R.; Shimodaira, Y.; Kudo, A. *Chem. Lett.* **2004**, *33*, 1348.
(43) Lim, A. R.; Choh, S. H.; Jang, M. S. *J. Phys.: Condens. Matter* **1995**, *7*, 7309.
(44) Bierlein, J. D.; Sleight, A. W. *Solid State Commun.* **1975**, *16*, 69.
(45) Kudo, A.; Omori, K.; Kato, H. *J. Am. Chem. Soc.* **1999**, *121*, 11459.
(46) Konta, R.; Ishii, T.; Kato, H.; Kudo, A. *J. Phys. Chem. B* **2004**, *108*, 8992.
(47) Kato, H.; Sasaki, Y.; Iwase, A.; Kudo, A. *Bull. Chem. Soc. Jpn.* **2007**, *80*, 2457.
(48) Sasaki, Y.; Nemoto, H.; Saito, K.; Kudo, A. *J. Phys. Chem. C* **2009**, *113*, 17536.
(49) Hara, S.; Irie, H. *Appl. Catal., B* **2012**, *115*−*116*, 330.
(50) Hara, S.; Yoshimizu, M.; Tanigawa, S.; Ni, L.; Ohtani, B.; Irie, H. *J. Phys. Chem. C* **2012**, *116*, 17458.
(51) Sayama, K.; Abe, R.; Arakawa, H.; Sugihara, H. *Catal. Commun.* **2006**, *7*, 96.
(52) Sasaki, Y.; Kato, H.; Kudo, A. *J. Am. Chem. Soc.* **2013**, *135*, 5441.
(53) Hitoki, G.; Takata, T.; Kondo, J. N.; Hara, M.; Kobayashi, H.; Domen, K. *Chem. Commun.* **2002**, 1698.
(54) Abe, R.; Takata, T.; Sugihara, H.; Domen, K. *Chem. Commun.* **2005**, 3829.
(55) Nakamura, R.; Tanaka, T.; Nakato, Y. *J. Phys. Chem. B* **2005**, *109*, 8920.
(56) Abe, R.; Higashi, M.; Domen, K. *ChemSusChem* **2011**, *4*, 228.
(57) Higashi, M.; Abe, R.; Ishikawa, A.; Takata, T.; Ohtani, B.; Domen, K. *Chem. Lett.* **2008**, *37*, 138.
(58) Maeda, K.; Abe, R.; Domen, K. *J. Phys. Chem. C* **2011**, *115*, 3057.
(59) Higashi, M.; Abe, R.; Teramura, K.; Takata, T.; Ohtani, B.; Domen, K. *Chem. Phys. Lett.* **2008**, *452*, 120.
(60) Higashi, M.; Abe, R.; Takata, T.; Domen, K. *Chem. Mater.* **2009**, *21*, 1543.
(61) Abe, R.; Takata, T.; Sugihara, H.; Domen, K. *Chem. Lett.* **2005**, *34*, 1162.
(62) Maeda, K.; Terashima, H.; Kase, K.; Higashi, M.; Tabata, M.; Domen, K. *Bull. Chem. Soc. Jpn.* **2008**, *81*, 927.
(63) Maeda, K.; Nishimura, N.; Domen, K. *Appl. Catal., A* **2009**, *370*, 88.
(64) Sasaki, R.; Maeda, K.; Kako, Y.; Domen, K. *Appl. Catal., B* **2012**, *128*, 72.
(65) Maeda, K.; Higashi, M.; Lu, D.; Abe, R.; Domen, K. *J. Am. Chem. Soc.* **2010**, *132*, 5858.
(66) Ma, S. S. K.; Maeda, K.; Domen, K. *Catal. Sci. Technol.* **2012**, *2*, 818.
(67) Matoba, T.; Maeda, K.; Domen, K. *Chem.—Eur. J.* **2011**, *17*, 14731.
(68) Grins, J.; Svensson, G. *Mater. Res. Bull.* **1994**, *29*, 801.
(69) Maeda, K.; Lu, D.; Domen, K. *ACS Catal.* **2013**, *4*, 1013.
(70) Ohno, T.; Tanigawa, F.; Fujihara, K.; Izumi, S.; Matsumura, M. *J. Photochem. Photobiol., A* **1998**, *118*, 41.
(71) Tabata, M.; Maeda, K.; Higashi, M.; Lu, D.; Takata, T.; Abe, R.; Domen, K. *Langmuir* **2010**, *26*, 9161.
(72) Dushman, P. *J. Phys. Chem.* **1904**, *8*, 481.
(73) Nozik, A. J. *Appl. Phys. Lett.* **1976**, *29*, 150.
(74) Kim, H. G.; Borse, P. H.; Choi, W.; Lee, J. S. *Angew. Chem., Int. Ed.* **2005**, *44*, 4585.
(75) Ma, S. S. K.; Maeda, K.; Hisatomi, T.; Tabata, M.; Domen, K. *Chem.—Eur. J.* **2013**, *19*, 7480.
(76) Iwase, A.; Ng, Y. H.; Ishiguro, Y.; Kudo, A.; Amal, R. *J. Am. Chem. Soc.* **2011**, *133*, 11054.
(77) Tsujiko, A.; Kisumi, T.; Magari, Y.; Murakoshi, K.; Nakato, Y. *J. Phys. Chem. B* **2000**, *104*, 4873.
(78) Ohno, T.; Sarukawa, K.; Matsumura, M. *New J. Chem.* **2002**, *26*, 1167.
(79) Ma, S. S. K.; Maeda, K.; Abe, R.; Domen, K. *Energy Environ. Sci* **2012**, *5*, 8390.
(80) Yamaguti, K.; Sato, S. *J. Chem. Soc., Faraday Trans. 1* **1985**, *81*, 1237.
(81) Maeda, K.; Teramura, K.; Lu, D.; Saito, N.; Inoue, Y.; Domen, K. *Angew. Chem., Int. Ed.* **2006**, *45*, 7806.
(82) Abe, R.; Sayama, K.; Arakawa, H. *Chem. Phys. Lett.* **2003**, *379*, 230.
(83) Sasaki, Y.; Iwase, A.; Kato, H.; Kudo, A. *J. Catal.* **2008**, *259*, 133.
(84) Tada, H.; Mitsui, T.; Kiyonaga, T.; Akita, T.; Tanaka, K. *Nat. Mater.* **2006**, *5*, 782.
(85) Wang, X.; Liu, G.; Chen, Z.-G.; Li, F.; Wang, L.; Lu, G. Q.; Cheng, H.-M. *Chem. Commun.* **2009**, 3452.
(86) Yu, Z. B.; Xie, Y. P.; Liu, G.; Lu, G. Q.; Ma, X. L.; Cheng, H.-M. *J. Mater. Chem. A* **2013**, *1*, 2773.
(87) Fu, N.; Jin, Z.; Wu, Y.; Lu, G.; Li, D. *J. Phys. Chem. C* **2011**, *115*, 8586.
(88) Tian, Y.; Tatsuma, T. *J. Am. Chem. Soc.* **2005**, *127*, 7632.
(89) Kowalska, E.; Abe, R.; Ohtani, B. *Chem. Commun.* **2009**, 241.
(90) Tanaka, A.; Hashimoto, K.; Kominami, H. *J. Am. Chem. Soc.* **2012**, *134*, 14526.
(91) Nishijima, Y.; Ueno, K.; Yokota, Y.; Murakoshi, K.; Misawa, H. *J. Phys. Chem. Lett.* **2010**, *1*, 2031.
(92) Nishijima, Y.; Ueno, K.; Kotake, Y.; Murakoshi, K.; Inoue, H.; Misawa, H. *J. Phys. Chem. Lett.* **2012**, *3*, 1248.
(93) Wang, X.; Li, S.; Ma, Y.; Yu, H.; Yu, J. *J. Phys. Chem. C* **2011**, *115*, 14648.
(94) Ye, L.; Liu, J.; Gong, C.; Tian, L.; Peng, T.; Zan, L. *ACS Catal.* **2012**, *2*, 1677.
(95) Takeda, H.; Ishitani, O. *Cood. Chem. Rev.* **2010**, *254*, 346.
(96) Sekizawa, K.; Maeda, K.; Domen, K.; Koike, K.; Ishitani, O. *J. Am. Chem. Soc.* **2013**, *135*, 4596.